

# PREPARATION BY ATOMIC LAYER DEPOSITION AND CHARACTERISATION OF CATALYST SUPPORTS SURFACED WITH ALUMINIUM NITRIDE

Riikka Puurunen

Dissertation for the degree of Doctor of Science in Technology to be presented with due permission of the Department of Chemical Technology for public examination and debate in Auditorium Ke 2 (Komppa-sali) at Helsinki University of Technology (Espoo, Finland) on the 25th of October, 2002, at 12 o'clock noon.

Helsinki University of Technology  
Department of Chemical Technology  
Laboratory of Industrial Chemistry

Teknillinen korkeakoulu  
Kemian tekniikan osasto  
Teknillisen kemian laboratorio

Distribution:

Helsinki University of Technology  
Laboratory of Industrial Chemistry  
P. O. Box 6100  
FIN-02015 HUT  
Tel. +358-9-451 2582  
Fax. +358-9-451 2622  
E-Mail: riikka.puurunen@hut.fi

© Riikka Puurunen

ISBN 951-22-6141-3 (print), 951-22-6142-1 (pdf, available at <http://lib.hut.fi/Diss/>)  
ISSN 1235-6840

Otamedia Oy  
Espoo 2002

# Preface

The work described in this thesis was carried out between January 1999 and October 2002 at the Laboratory of Industrial Chemistry, Helsinki University of Technology (HUT). The preparation of catalysts was carried out in the Surface Chemistry section of Fortum Oil and Gas Oy. Funding was provided by Fortum Oil and Gas Oy, by the National Technology Agency of Finland (TEKES) and by the Academy of Finland through the Graduate School in Chemical Engineering (GSCE) and a grant supporting work at the University of Leuven (K.U.Leuven, Belgium). The Emil Aaltonen Foundation and the Foundation of Technology (TES) provided personal grants.

I am most grateful to my supervisor, Professor Outi Krause, for her open-minded guidance of my research as well as for her straightforward comments. I also owe a deep debt of gratitude to Dr. Suvi Haukka and Dr. Marina Lindblad for all that they have taught me and for their enthusiastic interest in my doctoral work. My colleagues at HUT and Fortum are thanked for having provided friendly and fruitful working atmospheres.

During this work I have had the pleasure of working with many skillful scientists, without whom the comprehensive characterisation of the materials would not have been possible. I am greatly indebted to my coauthors Dr. Andrew Root and Dr. Priit Sarv for the NMR analyses, to Dr. Minna Viitanen and Professor Hidde Brongersma for the LEIS analyses, and to Mrs. Tarja Zeelie and Ms. Sanna Airaksinen for the catalytic activity measurements. The personnel at the Analytical Department of Fortum Oil and Gas Oy carried out the analyses skillfully and were always willing to pursue the analytical problems to a satisfactory conclusion. Mr. Jorma Hakala provided invaluable help with library services and Dr. Kathleen Ahonen by revising the language of this thesis and the appended publications.

Warmest thanks go to my family and friends for their support.

Espoo, October 2002,

Riikka Puurunen

“Tietä käyden tien on vanki.  
Vapaa on vain umpihanki.”

*Aaro Hellaakoski*

~ Following roads made by others may be easy, but not free.  
Making one's own roads, in turn, may be free, but never easy.

# Abstract

Catalyst supports with novel chemical and physical properties are needed for producing new families of catalytic materials. The goals of this work were to demonstrate the preparation of aluminium nitride type materials and evaluate their properties as catalyst supports.

To obtain aluminium nitride in high-surface-area form suitable for catalyst applications, porous silica and alumina supports were surfaced with aluminium nitride by the atomic layer deposition (ALD) technique by repeating the separate, saturating reactions of gaseous trimethylaluminium (TMA) and ammonia. The reaction temperatures of TMA and ammonia were 150 and 550 °C, respectively. Six reaction cycles led to an average growth of 2.4 aluminium atoms per cycle per square nanometre, and, according to low-energy ion scattering, 74% coverage. The aluminium nitride species were shown to be evenly distributed on the silica. The aluminium nitride appeared amorphous in X-ray diffraction, but  $^{27}\text{Al}$  nuclear magnetic resonance (NMR) spectroscopy confirmed its formation.

Insight into the growth mechanism of aluminium nitride was obtained by investigation of the individual steps leading to the growth. The surface reaction products after the TMA and ammonia reactions were identified by diffuse reflectance Fourier transform infrared spectroscopy and  $^1\text{H}$ ,  $^{13}\text{C}$  and  $^{29}\text{Si}$  NMR, and they were quantified by elemental analysis and  $^1\text{H}$  NMR. TMA reacted through ligand exchange with hydrogen atoms present on the surface in hydroxyl groups (OH) and amino groups ( $\text{NH}_x$ ), releasing methane, and further through dissociation in siloxane bridges, coordinatively unsaturated aluminium–oxygen pairs and nitrogen bridges. Steric hindrance imposed by the methyl ligands defined the saturation of the surface with adsorbed species; at saturation, there were five to six methyl groups per square nanometre. The ammonia reaction replaced the methyl groups present on TMA-modified surfaces with  $\text{NH}_x$  groups ( $x = 2, 1$  or  $0$ ). The results for the TMA reaction agreed quantitatively with the results obtained by others for the ALD growth of aluminium oxide thin films. A model was derived that relates the size and reactivity of the metal reactant to the growth per cycle of the oxide by ALD.

The properties of the AlN/oxide materials as catalyst supports were evaluated for cobalt hydroformylation and chromium dehydrogenation catalysts. In the preparation of the catalysts from cobalt(III) and chromium(III) acetylacetonate by ALD, the factor defining the saturation of the reaction was the same as on the respective oxides: the steric hindrance imposed by the acetylacetonate (acac) ligands. Dissociative and associative reactions of the metal acetylacetonate reactants and of the Hacac released in ligand exchange reaction took place on the AlN/oxide supports. This was a disadvantage for the Co/AlN/silica catalysts, as the high acac/Co ratio of the surface complex led to the desorption of cobalt(II) acetylacetonate during catalytic testing in hydroformylation.

After removal of the remaining acac ligands with ammonia, the activity of the Cr(III)/alumina and Cr(III)/AlN/alumina catalysts was evaluated in isobutane dehydrogenation at 580 °C. The aluminium nitride modification of the support decreased the dehydrogenation activity of the chromium catalysts. Pairs of chromium and oxygen ions seem to be required for active chromium catalysts, and replacing the neighbouring oxygen with nitrogen was a disadvantage.

Although no improvements were observed in catalytic performance of the prepared catalysts relative to conventional systems, the information obtained will be useful in the future investigations of the growth of aluminium nitride and of other materials by ALD and in the identification of the active sites on dehydrogenation catalysts.

# Tiivistelmä

Uudentyyppisten katalyyttisten materiaalien valmistuksessa tarvitaan kemiallisilta ja fysikaalisilta ominaisuuksiltaan entistä parempia katalyyttien kantajia. Tämän työn tavoitteena oli valmistaa alumiininitridityyppistä materiaalia ja arvioida valmistetun materiaalin soveltuvuus katalyyttien kantajaksi.

Alumiininitridiä valmistettiin huokoisten piidioksidin ja alumiinioksidin pintaan atomikerroskasvatustekniikalla (ALD), joka perustuu kaasumaisten lähtöaineiden kylästyviin, toisistaan erotettuihin reaktioihin kiinteän aineen pinnan kanssa. Lähtöaineina käytettiin trimetyylialumiinia (TMA) ja ammoniakkaa. TMA:n reaktiolämpötilaksi valittiin 150 °C ja ammoniakkin reaktiolämpötilaksi 550 °C. ALD-kasvatusta jatkettiin kuuden reaktiokierroksen ajan, jonka jälkeen peittoaste oli 74% matalan energian ionisironnalla määritettynä. Kasvu oli keskimäärin 2,4 alumiiniatomia neliönanometrillä reaktiokierrosta kohti. Alumiininitridiosalajit sijaitsivat tasaisesti piidioksidikantajan sisällä. Röntgendiffraktiossa ei näkynyt alumiininitridiä mutta  $^{27}\text{Al}$  ydinmagneettisen resonanssispektroskopian (NMR) perusteella alumiininitridiosalajeja muodostui.

Alumiininitridin kasvuun johtavia reaktiovaiheita tutkittiin selvittämällä TMA:n ja ammoniakkin reaktiossa muodostuneet pintatuotteet ja niiden määrät. Pintatuotteet selvitettiin diffuusirefleksansi Fourier-muunnos infrapunaspektroskopiolla sekä  $^1\text{H}$ ,  $^{13}\text{C}$  ja  $^{29}\text{Si}$  NMR -tekniikoilla. Pintatuotteiden määrät selvitettiin alkuainemäärityksin ja  $^1\text{H}$  NMR -tekniikalla. TMA reagoi ligandinvaihtoreaktiolla hydroksyyli- (OH) ja aminoryhmissä ( $\text{NH}_x$ ) olevien vetyatomien kanssa metaania vapauttaen, ja lisäksi se dissoitui siloksaanisiltoihin ja koordinaatiivisesti tyydyttymättömiin alumiini-happipareihin. Määräävä tekijä pinnan kyllästymisessä reaktiotuotteilla oli metyylliligandien aiheuttama steerinen estyminen; kyllästystilassa pinnalla oli viidestä kuuteen metyylliryhmää neliönanometrillä. Ammoniakki korvasi metyylliryhmät  $\text{NH}_x$ -ryhmillä ( $x = 2, 1$  tai  $0$ ). TMA:n reaktion osalta työn tulokset olivat yhdenmukaisia alumiinioksidiohukalvojen kasvatuksesta aiemmin saatujen tulosten kanssa. Työssä johdettiin malli, joka kuvaa metallilähtöaineen koon ja reaktiivisuuden vaikutusta oksidikasvatuksessa reaktiokierrosta kohti saatavaan kasvuun.

AlN/oksidi-materiaalien ominaisuuksia katalyyttien kantajana tutkittiin kobolttikatalyyteille hydroformyloinnissa ja kromikatalyyteille dehydruuksessa. Lähtöaineina katalyyttien valmistuksessa ALD-tekniikalla käytettiin koboltti(III)asetyyliasetonaattia ja kromi(III)asetyyliasetonaattia. Asetyyliasetonaattiligandien (acac) aiheuttama steerinen estyminen määräsi pinnan kyllästymisen reaktiotuotteilla. Metalliasetyyliasetonaattilähtöaineet sekä ligandinvaihtoreaktioissa vapautunut Hacac dissosioituivat ja assosioituivat AlN/oksidi-materiaalien pintaan. Tämä oli epäedullista Co/AlN/piidioksidi-katalyyteille, sillä korkeasta acac/Co-suhteesta johtuen koboltti(II)asetyyliasetonaattia haihtui pinnalta katalyyttien testauksen aikana.

Cr(III)/AlN/alumiinioksidi-katalyytit olivat aktiivisia isobutaanin dehydruuksessa 580 °C:ssa sen jälkeen kun acac-ligandit oli poistettu ammoniakikäsittelyllä. Alumiininitridin läsnäolo kantajan pinnassa laski kuitenkin katalyyttien dehydruusaktiivisuutta. Aktiivisissa kromikatalyyteissa tarvitaan ilmeisesti kromi-happipareja, eikä pariin kuuluvaa happea voi korvata tyrellä.

Vaikka tutkituilla katalyyteilla ei saatu korkeampaa aktiivisuutta kuin perinteisillä katalyyteilla, työssä saatua tietoa voidaan käyttää hyväksi alumiininitridin ja muiden materiaalien ALD-kasvumekanismien selvittämisessä sekä dehydruuskatalyyttien aktiivisen kohdan määrittämisessä.

# List of publications

This thesis is based on the following publications, which are referred to in the text by their Roman numerals:

- I Puurunen, R. L., Root, A., Haukka, S., Iiskola, E. I., Lindblad, M. and Krause, A. O. I.,  
IR and NMR study of the chemisorption of ammonia on trimethylaluminum-modified silica,  
*The Journal of Physical Chemistry B* **104** (2000) 6599–6609.
- II Puurunen, R. L., Root, A., Lindblad, M. and Krause, A. O. I.,  
Successive reactions of gaseous trimethylaluminium and ammonia on porous alumina,  
*Physical Chemistry Chemical Physics* **3** (2001) 1093–1102.
- III Puurunen, R. L., Root, A., Sarv, P., Haukka, S., Iiskola, E. I., Lindblad, M. and Krause, A. O. I.,  
Growth of aluminium nitride on porous silica by atomic layer chemical vapour deposition,  
*Applied Surface Science* **165** (2000) 193–202.
- IV Puurunen, R. L., Root, A., Sarv, P., Viitanen, M. M., Brongersma, H. H., Lindblad, M. and Krause, A. O. I.,  
Growth of aluminum nitride on porous alumina and silica through separate saturated gas–solid reactions of trimethylaluminum and ammonia,  
*Chemistry of Materials* **14** (2002) 720–729.
- V Rautiainen, A., Lindblad, M., Backman, L. B. and Puurunen, R. L.,  
Preparation of silica-supported cobalt catalysts through chemisorption of cobalt(II) and cobalt(III) acetylacetonate,  
*Physical Chemistry Chemical Physics* **4** (2002) 2466–2472.

- VI Puurunen, R. L., Zeelie, T. A. and Krause, A. O. I.,  
Cobalt(III) acetylacetonate chemisorbed on aluminium-nitride-modified silica: characteristics and hydroformylation activity,  
*Catalysis Letters*, in press.
- VII Puurunen, R. L., Airaksinen, S. M. K. and Krause, A. O. I.,  
Chromium(III) supported on aluminium-nitride-surfaced alumina: characteristics and dehydrogenation activity,  
*Journal of Catalysis*, in press.

Contribution of Riikka Puurunen to publications I–VII:

- I–IV She defined the research plan together with the coauthors, prepared all the samples, measured the DRIFT spectra, interpreted the results except the NMR and LEIS spectra, wrote the first version of the manuscript, and, after discussions with the coauthors, wrote the final version of the manuscript.
- V She designed and prepared part of the samples where  $\text{Co}(\text{acac})_3$  was reacted with bare silica, measured some DRIFT spectra, was a major contributor in interpreting the results of thermoanalysis and the reaction of  $\text{Co}(\text{acac})_3$  on silica, and, after discussions with the coauthors, wrote the final version of the manuscript.
- VI She designed and prepared the samples, measured the DRIFT spectra, interpreted the results relevant to the preparation of the catalysts, wrote the first version of the manuscript together with T. A. Zeelie, and, after discussions with the coauthors, wrote the final version of the manuscript.
- VII She designed and prepared the samples, measured the DRIFT spectra, interpreted the results relevant to the preparation of the catalysts, wrote the first version of the manuscript, and, after discussions with the coauthors, wrote the final version of the manuscript together with S. M. K. Airaksinen.

# Contents

<b>Preface</b>	<b>1</b>
<b>Abstract</b>	<b>3</b>
<b>Tiivistelmä</b>	<b>5</b>
<b>List of publications and author's contribution</b>	<b>7</b>
<b>Contents</b>	<b>9</b>
<b>1 Introduction</b>	<b>11</b>
<b>2 General background</b>	<b>13</b>
2.1 Atomic layer deposition (ALD) in catalyst preparation . . . . .	13
2.1.1 Basic principles . . . . .	13
2.1.2 Reactive sites on oxide supports . . . . .	16
2.1.3 Reaction mechanisms . . . . .	17
2.1.4 Means for controlling the metal content . . . . .	19
2.2 Catalytic hydroformylation . . . . .	19
2.3 Catalytic alkane dehydrogenation . . . . .	22
<b>3 Experimental</b>	<b>25</b>
3.1 Preparation of samples . . . . .	25
3.2 Characterisation of samples . . . . .	27
3.3 Evaluation of catalytic activity . . . . .	28
<b>4 Modification of porous oxides with aluminium nitride</b>	<b>30</b>
4.1 Reaction of trimethylaluminium (TMA) with silica and alumina . . . . .	30
4.1.1 Verification of surface saturation . . . . .	30
4.1.2 Reaction with OH groups and oxygen bridges . . . . .	31

4.1.3	Factor determining the surface saturation . . . . .	32
4.1.4	Growth of aluminium oxide from TMA and water by ALD . . . . .	33
4.1.5	Summary of the TMA reaction . . . . .	36
4.1.6	Relation of size and reactivity of $ML_n$ reactant to ALD growth of $MO_x$ material . . . . .	36
4.2	Reaction of ammonia with TMA-modified silica and alumina . . . . .	40
4.3	Repeated reactions of TMA and ammonia . . . . .	43
4.3.1	Deposition of aluminium nitride on silica and alumina . . . . .	43
4.3.2	Coverage of silica with aluminium nitride . . . . .	45
4.4	Comparison of ALD growth of aluminium nitride with growth of other materials . . . . .	46
<b>5</b>	<b>Cobalt/AlN/silica catalysts</b>	<b>49</b>
5.1	Reaction of $Co(acac)_3$ with silica and AlN/silica supports . . . . .	49
5.1.1	Verification of surface saturation . . . . .	49
5.1.2	Reaction mechanisms . . . . .	50
5.1.3	Factor determining the surface saturation . . . . .	51
5.1.4	Comparison with other saturating gas–solid reactions . . . . .	52
5.2	Hydroformylation activity . . . . .	53
<b>6</b>	<b>Chromium(III)/AlN/alumina catalysts</b>	<b>54</b>
6.1	Reaction of $Cr(acac)_3$ with alumina and AlN/alumina supports . . . . .	54
6.1.1	Verification of surface saturation . . . . .	54
6.1.2	Reaction mechanisms . . . . .	55
6.1.3	Factor determining the surface saturation . . . . .	56
6.1.4	Comparison with other saturating gas–solid reactions . . . . .	56
6.2	Dehydrogenation activity . . . . .	57
<b>7</b>	<b>Conclusions</b>	<b>59</b>
	<b>List of abbreviations and symbols</b>	<b>61</b>
	<b>References</b>	<b>64</b>
	<b>Appendices I–VII</b>	

# Chapter 1

## Introduction

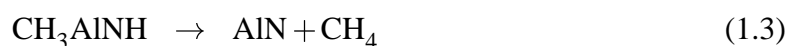
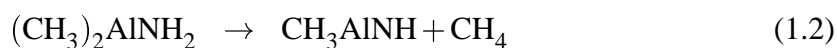
Oxide materials of porous structure, for example, silica and alumina, are used as supports for catalysts to provide a high surface area over which the catalytically active component is spread. Sometimes the catalyst support also stabilises structures of the catalyst material that are not stable in the bulk material but are crucial for catalytic activity.<sup>1</sup> In many cases the oxide supports catalyse side reactions, which are harmful for the selectivity of the process; for example, the acidic sites of an alumina support catalyse cracking.<sup>2</sup> With the ever-increasing demand for catalytic processes with high selectivities, which can minimise the amount of side products, alternative catalyst supports are being sought with improved chemical and physical properties.<sup>3–13</sup>

Nitrides are interesting candidates for catalyst supports. Metal nitrides have been successfully tested as catalyst supports in dehydrogenation,<sup>6–8</sup> hydrogenation,<sup>14</sup> dehydrocyclisation,<sup>15</sup> isomerisation,<sup>16</sup> hydroformylation,<sup>3</sup> vinylation<sup>17</sup> and oxidation.<sup>5</sup> The number of publications dealing with the use of metal nitrides as catalyst supports is limited, however, partly because of the difficulty of producing nitrides in porous high-surface-area forms suitable for catalyst application. Nitridation of metals or metal oxides with nitrogen or ammonia, which requires high temperatures, typically leads to nitrides of non-porous structure.<sup>18</sup> Ammonolysis of organometallic compounds or metal halides can lead to high surface areas (up to about  $300 \text{ m}^2 \text{ g}^{-1}$ ),<sup>8,19</sup> as, in favourable cases, can temperature programmed reaction of ammonia with porous metal oxides.<sup>4,20–22</sup> However, the structures of nitrides prepared by ammonolysis or temperature-programmed reaction are not always stable during the addition of the catalytically active metal.<sup>6–8</sup>

An alternative approach to the preparation of porous nitrides is to surface a (meso)porous oxide with a layer of the desired nitride. Preferably, the layer should be uniform in thickness and cover the support oxide fully. Atomic layer deposition (ALD), which involves repeating the separate, saturating gas–solid reactions of gaseous reactants

with a support,<sup>23–26</sup> is a technique potentially applicable for the preparation of such layer. The preparation of conformal oxide and nitride thin films on trenched surfaces by ALD has been demonstrated,<sup>27</sup> as has the preparation of several oxides on porous high-surface-area oxides.<sup>25,28–37</sup> This thesis summarises the first efforts to prepare aluminium nitride (AlN) on porous oxide supports by ALD.

Bulk aluminium nitride and aluminium nitride thin films can be prepared from ammonia and trimethylaluminium (TMA)<sup>19,38–52</sup> or aluminium trichloride.<sup>53</sup> Halide residues are undesired in many catalyst applications, and TMA and ammonia were chosen as reactants in this work. The preparation of aluminium nitride from TMA and ammonia proceeds via the types of reactions 1.1–1.3, where one methyl group at a time combines with a hydrogen atom of the ammonia molecule to release methane.



The specific goals of this work were to

- Demonstrate the preparation of aluminium nitride on porous silica and alumina supports by ALD from TMA and ammonia (III, IV). Before the processing of aluminium nitride, suitable reaction temperatures for TMA and ammonia were determined (I, II).
- Identify the factors determining the growth per cycle. This comprised (i) quantitative analysis of the reactive sites on the starting surfaces (I, II), (ii) identification and quantitative analysis of the surface reaction products (I–IV) and (iii) development of a model describing the TMA reaction (I, II).
- Evaluate the properties of the AlN/oxide materials as catalyst supports. Cobalt deposited on silica and AlN/silica supports was tested in hydroformylation (V, VI) and chromium deposited on alumina and AlN/alumina supports in dehydrogenation (VII).

# Chapter 2

## General background

This chapter describes the techniques and reactions that are dealt with in this thesis. Section 2.1 introduces the basic principles of preparing a catalyst by the ALD technique and reviews earlier investigations. The two processes where the AlN/oxide materials were investigated as catalyst supports, hydroformylation and dehydrogenation, are described in Sections 2.2 and 2.3, respectively.

### 2.1 Atomic layer deposition (ALD) in catalyst preparation

Atomic layer deposition was the key technique of this work. It was used to prepare aluminium nitride on porous silica and alumina (I–IV) and to deposit catalytically active components on the AlN/oxide supports (V–VII).

#### 2.1.1 Basic principles

The preparation of materials by ALD involves the following procedure:<sup>23–26</sup>

**Initiation:** Stabilisation of the reactive sites on the surface. This is typically carried out by a heat treatment. Physisorbed molecules, most often water adsorbed from ambient air, are removed.

**Step 1:** Saturating reaction of a gaseous reactant (reactant 1, typically a metal compound) with the reactive sites on the support surface. The reaction is allowed to proceed until the surface is saturated with the adsorbing species and no more reaction takes place. Thereafter, excess reactant and possible gaseous reaction products are removed by an inert gas purge or by evacuation.

Step 2: Saturating reaction of another reactant (reactant 2, typically a non-metal compound) with the reactive sites on the support. The adsorbed species left behind by the first reactant form a major part of the reactive sites. Excess reactant and the gaseous reaction products are removed.

Steps 1 and 2 are referred to as a reaction cycle and are repeated to increase the amount of adsorbed species. A schematic illustration of one reaction cycle is shown in Figure 2.1. In thin film growth, one reaction cycle is accomplished in seconds, and the reactions of the metal reactant and the non-metal reactant are performed at the same temperature. In the processing of porous materials with large surface areas, longer reactant exposures, typically hours, are required. The longer times allow different reaction temperatures to be used for the two reactants. Organometallic compounds and metal halides,  $\beta$ -diketonates and alkoxides are most commonly applied as metal reactants, and non-metal hydrides ( $\text{H}_2\text{O}$ ,  $\text{NH}_3$  and  $\text{H}_2\text{S}$ ) are typically used as non-metal reactants.<sup>23–26</sup> The non-metal hydrides are not always sufficiently reactive to enable ligand removal (Step 2), and oxidising agents, such as oxygen and ozone, have been used instead.<sup>23–26</sup>

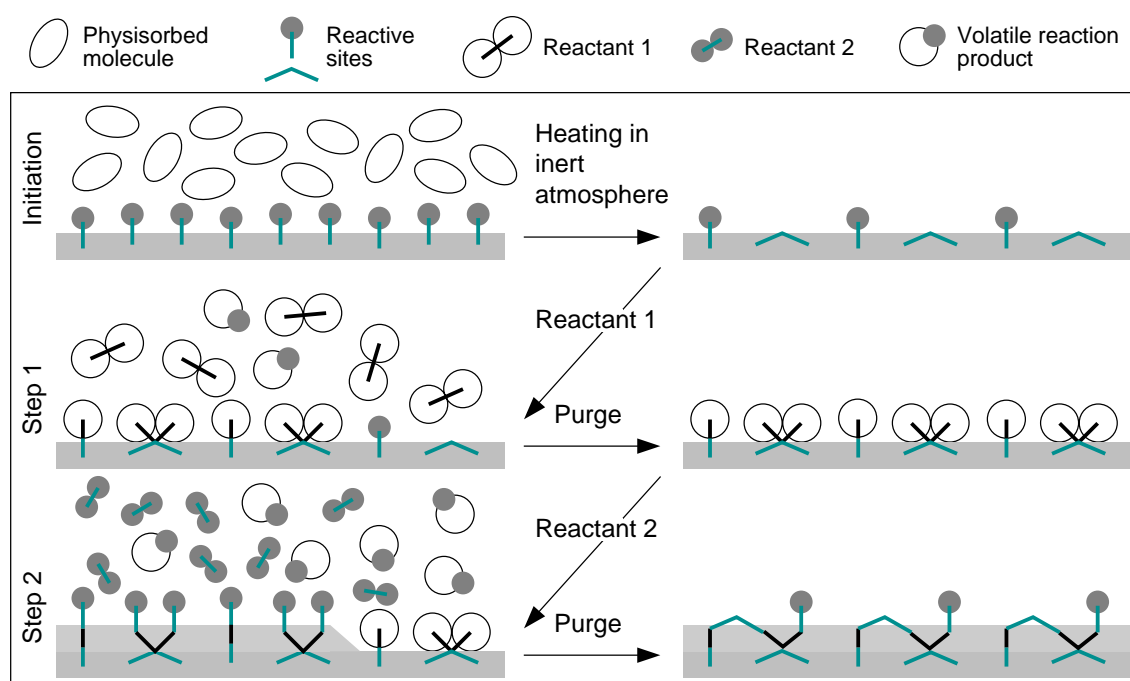


**Figure 2.1:** Schematic illustration of the steps leading to growth of  $\text{MZ}_x$  materials (M denotes metal, Z non-metal) by ALD. The surface sites that are not accessible to the reactants because of steric constraints are omitted for simplicity.

To achieve conditions where gas–solid reactions are saturating, reactants and reaction temperatures are selected where physisorption of the reactants and thermal decomposition are eliminated by sufficiently high temperature and sufficiently low temperature. Under these conditions, the gas–solid reactions proceed only as long as there are sterically available, sufficiently reactive sites available on the surface.

Active catalysts have been produced by ALD for a variety of purposes, as shown in Table 2.1. Sometimes, catalysts can be prepared in just one reaction cycle,<sup>54,55</sup> but often it is desirable to increase the concentration of the metal compound by repeating the reaction cycles of the metal and the non-metal reactant.<sup>30,35</sup>

**Table 2.1:** Examples of reactions for which catalysts have been prepared by ALD and description of the catalyst.

Reaction	Catalyst	Support	Reactants	Refs.
Alkane dehydrogenation	CrO <sub>x</sub>	Alumina	Cr(acac) <sub>3</sub> , <sup>a</sup> air	30, 37, 56
	VO <sub>x</sub>	Silica, alumina	VO(acac) <sub>2</sub> , air	55, 57
Ethene hydroformylation	Co	Silica	Co(acac) <sub>3</sub> , air	54
Toluene hydrogenation	Ni	Alumina	Ni(acac) <sub>2</sub> , air	29, 58
	Co	Silica	Co(acac) <sub>3</sub> , air <sup>b</sup>	35, 59, 60
	Co	Alumina	Co(acac) <sub>2</sub> , air <sup>b</sup>	59
Alkene metathesis	WO <sub>x</sub>	Silica, alumina,	WOCl <sub>4</sub> or	61
		magnesia	WCl <sub>6</sub> , air	
Methane oxidation	CoO <sub>x</sub>	Zirconia	Co(acac) <sub>3</sub> , air <sup>b</sup>	62
Methanol oxidation	TaO <sub>x</sub>	Silica, alumina,	Ta(OC <sub>2</sub> H <sub>5</sub> ) <sub>5</sub> , air	63
		zirconia		
	VO <sub>x</sub>	Silica, alumina,	VO(acac) <sub>2</sub> , air	63
		zirconia		
Alkene polymerisation	CrO <sub>x</sub>	Silica	Cr(acac) <sub>3</sub> , air	64
	CrO <sub>x</sub>	Silica	CrO <sub>2</sub> Cl <sub>2</sub>	65
Alcohol dehydration	ZrO <sub>2</sub>	Alumina	ZrCl <sub>4</sub> , H <sub>2</sub> O	66

<sup>a</sup> Acac = acetylacetonate. <sup>b</sup> Catalysts with higher activity were produced by omitting the ligand removal with air.<sup>35</sup>

Several terms are used in the literature to describe processes that are based on repeating separate, saturating gas–solid reactions. In addition to ALD, terms such as atomic layer epitaxy (ALE),<sup>23–25,55</sup> atomic layer chemical vapour deposition (ALCVD<sup>TM</sup>),<sup>67</sup> molecular layering,<sup>68</sup> atomic layer growth,<sup>49</sup> atomic layer processing<sup>69</sup> and chemical surface coating<sup>70</sup> can be found. Atomic layer epitaxy was the original term, used by

Suntola and co-workers, who developed the technique in the 70's for the preparation of ZnS thin films for electroluminescent devices.<sup>71</sup> During the 90's, the ALE technique was extended to catalyst preparation.<sup>24,25,28,72</sup> In catalyst applications, and most often also in thin film applications, the processed materials are amorphous or polycrystalline, not epitaxial, in nature,<sup>23,25,26,73</sup> and the original term, atomic layer epitaxy, does not well describe the processed materials. Although the term atomic layer deposition is now preferred,<sup>26,56,57,63,74,75</sup> some groups<sup>66,76</sup> prefer to use the original term, mainly for historical reasons.<sup>76</sup> In this thesis, the term atomic layer deposition (ALD) is used.

## 2.1.2 Reactive sites on oxide supports

Since the reactive sites on the support are responsible for bonding the gaseous reactants, understanding their nature is of great importance for ALD processing. Three main types of reactive sites have been identified on oxide surfaces: hydroxyl (OH) groups, coordinatively unsaturated (c.u.s.) sites and oxygen bridges.<sup>2,77-80</sup> OH groups can further be classified according to the extent of hydrogen bonding or basicity.<sup>2,77-80</sup>

In ambient conditions, the surfaces of oxide materials are terminated with OH groups, and further covered by layers of physisorbed water. Before the preparation of catalysts by ALD, physisorbed water must be removed. Furthermore, the number of remaining OH groups is typically stabilised to the desired level by heating the support in an inert atmosphere. Heating the surface leads to dehydroxylation, that is, neighbouring OH groups condense to release water. As illustrated in Figure 2.2, on silica, dehydroxylation leads to the formation of siloxane bridges, whereas on alumina it leads to coordinatively unsaturated (c.u.s.) Al–O pairs. Siloxane bridges and c.u.s. Al–O pairs are referred to in this thesis as oxygen bridges.



**Figure 2.2:** Schematic presentation of dehydroxylation: (A) the formation of siloxane bridges on silica and (B) the formation of c.u.s. Al–O pairs on alumina.

The amount of OH groups remaining after heat-treatment, at a certain temperature, sufficiently long to stabilise the surface is characteristic for the oxide in question. The amounts of OH groups remaining on silica and alumina supports, as determined by others<sup>77</sup> and in this work by <sup>1</sup>H magic-angle spinning nuclear magnetic resonance (MAS NMR) spectroscopy (I, II), are shown in Figure 2.3. The OH group content is somewhat

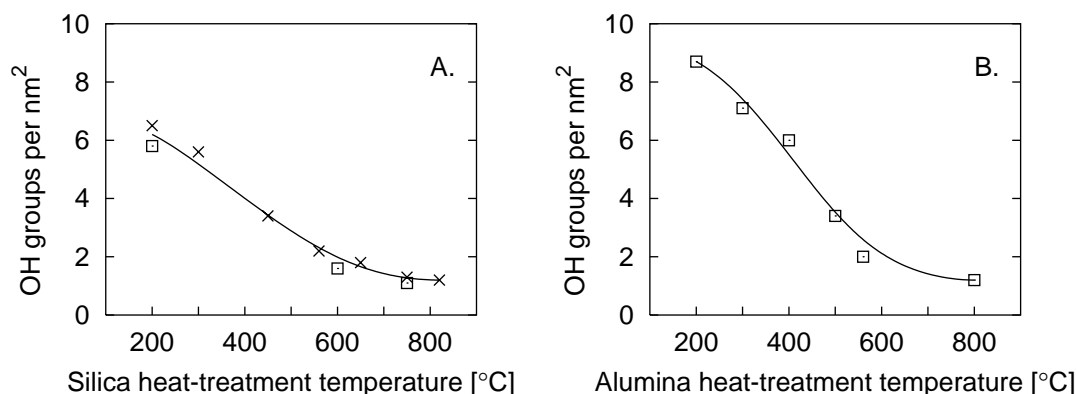


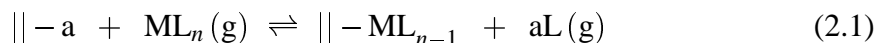
**Figure 2.3:** The amount of OH groups (A) on silica and (B) on alumina as a function of the heat-treatment temperature, determined by  $^1\text{H}$  MAS NMR. Crosses (A) show the values determined by Haukka et al.<sup>77</sup> and squares (A,B) the results of this work (I,II,V).

lower on silica than on alumina up to heating at about 550 °C; beyond this the OH group contents on silica and alumina are the same.

### 2.1.3 Reaction mechanisms

The mechanisms that have been identified for bonding gaseous reactants on solid supports in a saturating manner are illustrated with molecule  $\text{ML}_n$  used as an example. In  $\text{ML}_n$ , M is a central metal atom, L is a ligand attached to it and  $n$  is the number of ligands. Thus,  $\text{ML}_n$  can represent  $\text{AlMe}_3$  (Me = methyl),  $\text{Cr}(\text{acac})_3$  (acac = acetylacetonate) and  $\text{ZrCl}_4$  molecules. Similar reactions can be identified for non-metal hydrides (e.g.,  $\text{H}_2\text{O}$ ,  $\text{NH}_3$  and  $\text{H}_2\text{S}$ ). Oxidations and reactions of atomic reactants such as vaporised metals are not discussed here.

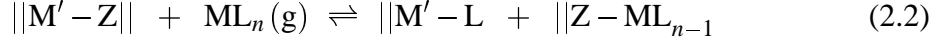
The most common example of saturating gas–solid reactions is ligand exchange reaction (2.1), where the reactant molecule ( $\text{ML}_n$ ) is split and one of its ligands (L) combines with a surface group (a) to form a volatile compound that is released as a gaseous reaction product (aL).



Symbol || denotes the surface. Ligand exchange reaction (2.1) has been shown to occur, for example, between hydrogen atoms present in surface OH groups and  $\text{AlMe}_3$ ,<sup>81–83</sup>  $\text{Cr}(\text{acac})_3$ <sup>84,85</sup> and  $\text{ZrCl}_4$ .<sup>31,80</sup> It is often considered as the preferable reaction mechanism in catalyst preparation because the equilibrium can be directed towards the products through removal of the gaseous reaction products.<sup>25</sup>

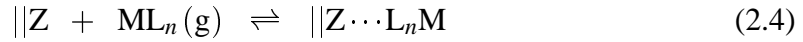
Dissociative adsorption (2.2), which is another example of saturating gas–solid re-

actions, involves the splitting of the reactant molecule onto coordinatively unsaturated (c.u.s.) sites or oxygen bridges on a surface, with both parts of the molecule bonded to the surface.



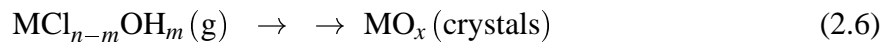
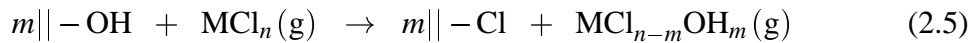
$M'$  denotes a cation, such as silicon or aluminium, and  $Z$  denotes an anion, such as oxygen. Dissociation (2.2) is proposed to take place, for instance, between the c.u.s. sites on alumina and  $Cr(acac)_3$ <sup>37</sup> or  $ZrCl_4$ .<sup>80</sup> Siloxane bridges are less reactive than the c.u.s. sites: for example,  $Cr(acac)_3$  and  $ZrCl_4$  do not dissociate into them.<sup>80,84-86</sup> However, some highly reactive compounds, such as  $AlMe_3$ ,<sup>81-83</sup> are able to dissociate into siloxane bridges.

Associative adsorption can also be saturating, provided that it involves the formation of a site-specific bond between the reactant and the surface and can thus be classified as chemisorption. Two types of saturating associative reactions have been identified: association through the central atom (2.3) and association through the ligands (2.4).



$ZnCl_2$ , for example, adsorbs on a  $ZnS$  surface through an interaction between the central zinc atom and a surface sulphur atom,<sup>87</sup> which is type 2.3 association. The adsorption of  $Cr(acac)_3$  on silica and alumina at 160–190 °C, in turn, has been concluded to occur through saturating associative adsorption between the acac ligands and surface OH groups,<sup>85,86,88</sup> which is type 2.4 association. Whether associative adsorption is chemisorption or physisorption depends on the reaction temperature: for example, adsorption of  $Cr(acac)_3$  at 130 °C is not saturating and leads to multilayer formation,<sup>89</sup> which is characteristic for physisorption.

A special class of saturating gas–solid reactions has been identified for metal chloride reactants on oxide surfaces.<sup>31,80,90-93</sup> Metal halide reactants in general might follow this reaction path. Metal chlorides can exchange part of their chloride ligands with surface OH groups in a reaction referred to as chlorination (2.5), forming intermediate volatile oxychloride species.<sup>90,91</sup> These intermediate species facilitate the agglomeration process (2.6), which already in the first reaction cycle may lead to the formation of metal oxide crystallites, visible in X-ray diffraction (XRD).<sup>90,91</sup>



The details of the agglomeration process have not been described.<sup>91,93</sup> Despite the agglomeration, the reactions of metal chlorides on oxide surfaces have been concluded to

be saturating in nature.<sup>31,80,90–93</sup>

#### 2.1.4 Means for controlling the metal content

When the surface has been saturated with adsorbed species of reactant  $ML_n$ , there are two factors that mostly affect the element contents: (i) the number of bonding sites on the starting surface and (ii) steric effects associated with the ligands.<sup>23–26</sup> Table 2.2 summarises the results of investigations where the amounts of metal and ligand attached have been measured as a function of the heat-treatment temperature of the support. Clearly, increase in the support heat-treatment temperature, that is, decrease in the number of OH groups, typically decreases the content of bonded metal. Increase in the size of ligands also can decrease the amount of bonded metal. This has been shown, for example, for the deposition of nickel on alumina from  $Ni(acac)_2$  and  $Ni(thd)_2$  ( $thd = 2,2,6,6$ -tetramethyl-3,5-heptanedionate), where the larger  $thd$  ligands resulted in a smaller nickel content (2.3 vs.  $0.92 \text{ at}_{Ni} \text{ nm}^{-2}$ ).<sup>24</sup> Further decrease in the amount of bonded metal can be achieved by selective blocking of part of the reactive sites on the surface.<sup>30,84</sup>

It is also possible to affect the metal content at saturation through the choice of reaction temperature. However, the effect of reaction temperature is rather unpredictable and depends on the reactant–support pair. With increasing reaction temperature, the amount of deposited metal may increase [as observed for the  $Cr(acac)_3$ –silica,<sup>84</sup>  $La(thd)_3$ –silica<sup>25,33</sup> and titanium isopropoxide ( $Ti(OPr^i)_4$ )–alumina<sup>32</sup> reactions], stay constant [as observed for the  $Ti(OPr^i)_4$ –silica<sup>32</sup> reaction] or decrease [as observed for the  $TiCl_4$ –silica,<sup>90,91</sup>  $ZrCl_4$ –silica<sup>80</sup> and  $ZrCl_4$ –alumina<sup>80</sup> reactions].

If higher metal contents are desired than are achieved in a single saturating reaction, reaction cycles of the metal reactant and a non-metal reactant can be repeated. Table 2.3 summarises investigations where more than one reaction cycle of metal reactant deposition and ligand removal was carried out. Average values of growth per cycle are also given in Table 2.3. Typically, the metal content increases more or less linearly with the number of reaction cycles.<sup>25,33</sup> However, there have been exceptions, such as the  $Cu(thd)_2$ – $O_2$ /silica process<sup>25,33</sup> and the  $TiCl_4$ – $H_2O$ /silica process,<sup>28</sup> where less metal is deposited per cycle with increasing number of reaction cycles.

## 2.2 Catalytic hydroformylation

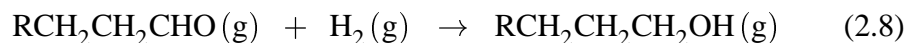
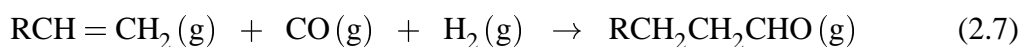
The activity of cobalt catalysts prepared on AlN/silica samples was evaluated in ethene hydroformylation (VI). In hydroformylation, alkenes are converted with carbon monoxide and hydrogen into aldehydes (2.7) and alcohols (2.8), which are used as intermediates in

**Table 2.2:** Examples of investigations where the saturating reaction of a metal compound has been investigated as a function of the support heat-treatment temperature.

Reactant/support, reaction temperature	Support heat- treatment temperature	Metal atoms per nm <sup>2</sup>	Ratio of ligand to metal	Ligands per nm <sup>2</sup>	Refs.
Cr(acac) <sub>3</sub> /silica, 160 °C	200→820 °C	0.7→0.5	3 <sup>a</sup>	2.1→1.5	85
Cr(acac) <sub>3</sub> /silica, 190 °C	200→800 °C	0.8→0.6	3 <sup>a</sup>	2.4→1.8	86
Cr(acac) <sub>3</sub> /silica, 200 °C	200→820 °C	0.8→0.3	2 <sup>a</sup>	1.4→0.6	84,85
Cr(acac) <sub>3</sub> /alumina, 190 °C	200→800 °C	0.7 <sup>a</sup>	3 <sup>a</sup>	2.2 <sup>a</sup>	88
Ni(acac) <sub>2</sub> /alumina, 200 °C	200→800 °C	2.5→2.0	5→8	2.5→3.2	29
Ce(thd) <sub>4</sub> /silica, 220 °C	200→820 °C	0.9→0.5	1.4→2.8	1.3→1.4	33
Mn(thd) <sub>3</sub> /silica, 180 °C	200→820 °C	1.1→0.7	<sup>b</sup>	<sup>b</sup>	25
La(thd) <sub>3</sub> /silica, 180 °C	200→820 °C	1.3→0.7	<sup>b</sup>	<sup>b</sup>	25
Y(thd) <sub>3</sub> /silica, 200 °C	200→820 °C	0.8→0.6	1.3→1.8	1.1 <sup>a</sup>	94
TiCl <sub>4</sub> /silica, 175 °C	200→820 °C	2.0→0.7	2.4→3.0	4.8→2.1	90
TiCl <sub>4</sub> /silica, 450 °C	450→820 °C	1.1→0.5	2 <sup>a</sup>	2.2→0.9	90
TiCl <sub>4</sub> /silica, 550 °C	560→820 °C	0.8→0.4	2.3 <sup>a</sup>	1.8→0.9	91
ZrCl <sub>4</sub> /silica, 300 °C	300→600 °C	1.7→1.0	2.6→2.3	4.4→2.3	80
ZrCl <sub>4</sub> /alumina, 300 °C	300→600 °C	1.9→1.5	2.8→3.1	5.3→4.9	80
AlMe <sub>3</sub> /silica, 200 °C	300→900 °C	3.2→1.0	2.4→2.6	7.7→2.6	83
AlMe <sub>3</sub> /silica, 250 °C	350→600 °C	3.6→2.6	1.7→2.2	6.1→5.7	95
HMDS/alumina, 200 °C <sup>c</sup>	200→600 °C	1.5 <sup>a,c</sup>	3 <sup>a,c</sup>	4.5 <sup>a,c</sup>	34

<sup>a</sup> The value remains constant. <sup>b</sup> Not reported. <sup>c</sup> HMDS = Hexamethyldisilazane, ((CH)<sub>3</sub>Si)<sub>2</sub>NH. Metal refers to Si and ligand to Me groups.

the production of a variety of oxygen-containing chemicals.<sup>96</sup>



The catalyst is typically a cobalt or rhodium complex.<sup>96</sup> For homogeneous liquid-phase cobalt catalysts, operation conditions are most often 160–180 °C and 10–30 MPa.<sup>96</sup> The reaction takes place in four steps:<sup>96</sup> (i) formation of cobalt hydride, CoH; (ii) addition of alkene to the Co–H bond, producing Co–R'; (iii) insertion of CO into the Co–R' bond, producing Co–C(O)–R'; and (iv) reductive cleavage of the Co–C bond by H<sub>2</sub>, producing R'CHO and regenerating CoH.

Separation of the catalyst complex from the reaction products is a serious problem in conventional homogeneous hydroformylation.<sup>96–99</sup> Heterogeneous hydroformylation

**Table 2.3:** Summary of the ALD growth of various oxides ( $\text{MO}_x$ ) on porous oxide supports.

$\text{MO}_x$	Support (heat-treatment temp., °C)	Reaction 1		Reaction 2		Cycles		Refs.
		Reactant 1	Temp. 1, °C	Reactant 2	Temp. 2, °C	No.	$\text{at}_M \text{ nm}^{-2}$ per cycle	
$\text{TiO}_2$	Silica (450)	$\text{TiCl}_4$	450	$\text{H}_2\text{O}$	450	4	0.6	28
$\text{TiO}_2$	Silica (400)	$\text{TiCl}_4$	25	$\text{H}_2\text{O}$	100	8	1.5 <sup>a</sup>	36
$\text{TiO}_2$	Silica (450)	$\text{Ti}(\text{OPr}^i)_4$	160	$\text{O}_2$	450	5	1.0	32
$\text{TiO}_2$	Alumina (600)	$\text{Ti}(\text{OPr}^i)_4$	100	$\text{O}_2$	450	5	1.0	32
$\text{NiO}$	Alumina (800)	$\text{Ni}(\text{acac})_2$	200	$\text{O}_2$	400	10	1.9	29
$\text{Al}_2\text{O}_3$	Silica (600)	$\text{AlMe}_3$	120	$\text{H}_2\text{O}$	120	5	0.9 <sup>b</sup>	83
$\text{CrO}_x$	Alumina (600)	$\text{Cr}(\text{acac})_3$	200	$\text{O}_2$	600	10	0.8	30,37
$\text{ZrO}_2$	Silica (300)	$\text{ZrCl}_4$	300	$\text{H}_2\text{O}$	300	5	0.9	31
$\text{ZrO}_2$	Alumina (600)	$\text{ZrCl}_4$	300	$\text{H}_2\text{O}$	600	5	1.0	31
$\text{LaO}_x$	Alumina	$\text{La}(\text{thd})_3$	240	$\text{O}_2$	400–600 <sup>25</sup>	4	0.6	25,33
$\text{YO}_x$	Silica (500)	$\text{Y}(\text{thd})_3$	225	$\text{O}_2$	480	5	0.5	94
$\text{CeO}_x$	Alumina	$\text{Ce}(\text{thd})_4$	220	$\text{O}_2$	400–600 <sup>25</sup>	4	0.4	25,33
$\text{CuO}$	Silica	$\text{Cu}(\text{thd})_2$	170	$\text{O}_2$	400–600 <sup>25</sup>	4	0.3	25,33
$\text{CuO}$	Alumina	$\text{Cu}(\text{thd})_2$	170	$\text{O}_2$	400–600 <sup>25</sup>	4	0.5	25,33
$\text{SiO}_x$	Alumina (600)	HMDS	200	$\text{O}_2$	500–550	8	1.5	34
$\text{CoO}_x$	Silica (600)	$\text{Co}(\text{acac})_3$	180	$\text{O}_2$	450	5	1.6	35,59 60, V
$\text{CoO}_x$	Alumina (875)	$\text{Co}(\text{acac})_2$	180	$\text{O}_2$	450	5	1.5	59
$\text{CoO}_x$	Zirconia (600)	$\text{Co}(\text{acac})_3$	170	$\text{O}_2$	500	5	1.3	62

<sup>a</sup> Deposition of about  $2.2 \text{ at}_{\text{Ti}} \text{ nm}^{-2}$  during first six cycles, thereafter no further increase.

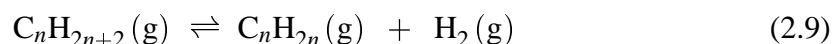
<sup>b</sup> Deposition of  $2.8 \text{ at}_{\text{Al}} \text{ nm}^{-2}$  in the first cycle, thereafter about  $0.4 \text{ at}_{\text{Al}} \text{ nm}^{-2}$  per cycle.

catalysts have been introduced as a way to overcome this problem.<sup>96–99</sup> In liquid phase, the metal in heterogeneous catalysts may leach from the support, however,<sup>100</sup> and heterogeneous catalysts are more feasibly used in gas phase, where no leaching has been

observed.<sup>54</sup> Cobalt catalysts supported on silica by the saturating gas–solid reaction of  $\text{Co}(\text{acac})_3$  have shown higher selectivity in hydroformylation than similar catalysts prepared by impregnation.<sup>54</sup> The higher activity is explained by the high dispersion of cobalt in catalysts prepared from  $\text{Co}(\text{acac})_3$  through gas phase; the CO insertion needed for aldehyde production is favoured on isolated metal sites.<sup>101,102</sup> Lower dispersion and larger particle size of cobalt, in turn, lead to increased hydrogenation activity, which is disadvantageous for hydroformylation.<sup>96</sup>

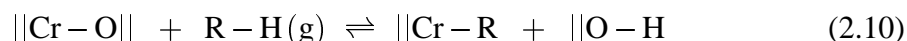
## 2.3 Catalytic alkane dehydrogenation

The activity of chromium catalysts prepared on AlN/alumina samples was evaluated in isobutane dehydrogenation (VII). In dehydrogenation, short-chain alkanes are converted to higher-value alkenes and hydrogen (2.9).<sup>103</sup>



Dehydrogenation is an endothermic process and limited by thermodynamic equilibrium.<sup>103</sup> To achieve high conversions requires high temperatures and low partial pressures. Higher conversions may also be achieved by separating hydrogen from the product stream, for example, by membranes.<sup>104,105</sup>

The catalyst is typically chromia or platinum–tin supported on alumina and promoted by alkali metals.<sup>103</sup> For chromia catalysts, the operation temperatures and pressures depend on the process, but are about 600 °C and 30–150 kPa.<sup>103</sup> Dehydrogenation is suggested to involve a step where the alkane dissociates to a pair of chromium and oxygen ions, to give a hydrogen atom bonded to surface oxygen and an alkyl group bonded to surface chromium (2.10).<sup>106–108</sup>



The dissociation of alkane has been suggested to be the rate limiting step in dehydrogenation.<sup>109,110</sup>

Most of the chromium in calcined chromia/alumina catalysts is present in oxidation states  $\text{Cr}^{3+}$  and  $\text{Cr}^{6+}$ , although some  $\text{Cr}^{2+}$  and  $\text{Cr}^{5+}$  may be present as well.<sup>1</sup> Figure 2.4 summarises the types of  $\text{Cr}^{6+}$  and  $\text{Cr}^{3+}$  species found over a wide range of chromium concentrations.<sup>37,111–114</sup> Comparison of the results not given as surface loadings,  $c_{\text{Cr}}$  [ $\text{at}_{\text{Cr}}\text{nm}^{-2}$ ], required conversion of the chromium contents in the original articles according to equation

$$c_{\text{Cr}} = \frac{c_{\text{Cr}}^{\text{wt}\%} N_{\text{A}}}{100S} \left( M_{\text{Cr}} - \frac{1}{100} c_{\text{Cr}}^{\text{wt}\%} M_{\text{CrO}_x} \right)^{-1}, \quad (2.11)$$

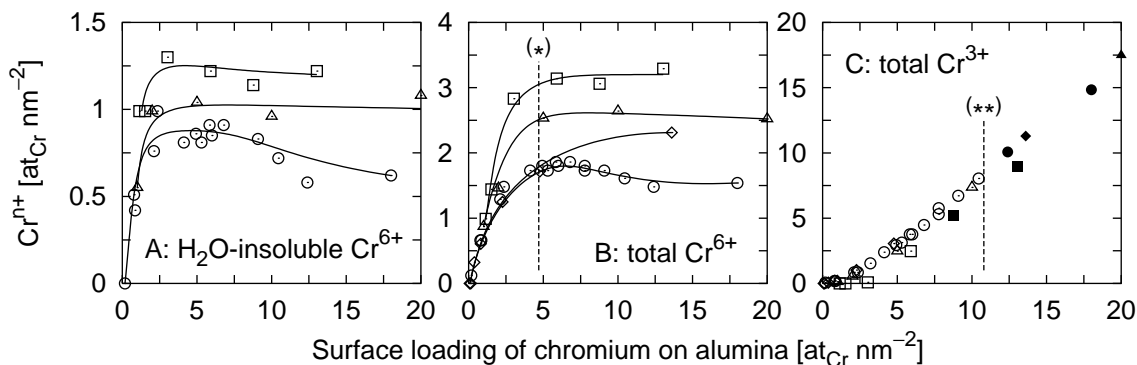


**Figure 2.4:** Summary of the Cr<sup>6+</sup> and Cr<sup>3+</sup> species present on oxidised chromia/alumina catalysts: (A) H<sub>2</sub>O-insoluble Cr<sup>6+</sup>, (B) total Cr<sup>6+</sup> and (C) total Cr<sup>3+</sup>. Note that the y-axes in (A), (B) and (C) differ in scale. The experimental points of Hakuli et al.<sup>37,111</sup> are shown in circles, Grzybowska et al.<sup>112</sup> in triangles, Cavani et al.<sup>113</sup> in squares and De Rossi et al.<sup>114</sup> in diamonds. The lines marked with (\*) and (\*\*) show the surface concentration of chromium on CrO<sub>3</sub> and Cr<sub>2</sub>O<sub>3</sub>, respectively.<sup>112,115</sup> Full symbols in (C) indicate that Cr<sub>2</sub>O<sub>3</sub> crystallites have been detected in XRD.

where  $c_{\text{Cr}}^{\text{wt}\%}$  denotes the concentration of chromium [wt%],  $N_{\text{A}}$  is Avogadro's number,  $S$  is the surface area reported for the alumina support [ $\text{m}^2 \text{g}^{-1}$ ],  $M_i$  is the molar mass of component  $i$  [ $\text{g mol}^{-1}$ ], and  $x$  was assumed to be 1.5, corresponding to chromium in Cr<sub>2</sub>O<sub>3</sub>. The Cr<sup>6+</sup> content initially increases with chromium loading, until the amount of H<sub>2</sub>O-insoluble Cr<sup>6+</sup>, which is directly grafted to alumina,<sup>113</sup> stabilises to about 1  $\text{at}_{\text{Cr}} \text{nm}^{-2}$  by a chromium loading of about 2  $\text{at}_{\text{Cr}} \text{nm}^{-2}$ , and the total amount of Cr<sup>6+</sup> stabilises to about 2–3  $\text{at}_{\text{Cr}} \text{nm}^{-2}$  by a chromium loading of 5  $\text{at}_{\text{Cr}} \text{nm}^{-2}$ . The amount of Cr<sup>3+</sup> increases steadily with chromium loading, and Cr<sub>2</sub>O<sub>3</sub> crystallites are observed in XRD for chromium loadings of about 12  $\text{at}_{\text{Cr}} \text{nm}^{-2}$  and beyond.

After the reduction of chromia/alumina catalysts during dehydrogenation with hydrogen or alkane, Cr<sup>3+</sup> is the major oxidation state,<sup>37,56,107,111,113,114,116–120</sup> although part of the chromium may reduce to Cr<sup>2+</sup> and, after reduction with hydrogen, some Cr<sup>5+</sup> may remain.<sup>120,121</sup> Dehydrogenation activity of chromia/alumina catalysts is most often attributed to coordinatively unsaturated Cr<sup>3+</sup> ions.<sup>37,56,106,107,111,113,114,119</sup> The types of Cr<sup>3+</sup> sites that are most active are under debate, however: De Rossi et al.<sup>107,114</sup> and Hakuli et al.<sup>111</sup> have proposed mononuclear redox Cr<sup>3+</sup> to be the active site (redox Cr<sup>3+</sup> referring to Cr<sup>3+</sup> formed through reduction of chromium from higher oxidation states), whereas Cavani et al.,<sup>113</sup> Airaksinen et al.<sup>56</sup> and Puurunen and Weckhuysen<sup>119</sup> have concluded that non-redox Cr<sup>3+</sup>, that is, clustered Cr<sup>3+</sup>,<sup>119</sup> is more active. One reason for

the apparent disagreement may be the small number of investigations carried out on catalysts with higher chromium loadings. Reportedly,<sup>37,113</sup> the dehydrogenation activity is maximum at a chromium surface loading of 10–12  $\text{at}_{\text{Cr}} \text{nm}^{-2}$ ; industrial catalysts contain about 15  $\text{at}_{\text{Cr}} \text{nm}^{-2}$ .<sup>103</sup> Hakuli et al.<sup>37,116</sup> have shown that, above a surface loading of 5  $\text{at}_{\text{Cr}} \text{nm}^{-2}$ , redox  $\text{Cr}^{3+}$  sites alone cannot account for the activity.

# Chapter 3

## Experimental

This chapter summarises briefly the investigations that were carried out. Full experimental details can be found in publications I–VII.

### 3.1 Preparation of samples

Porous silica and alumina were modified with aluminium nitride and cobalt and chromium were supported on the oxide and AlN/oxide materials (the oxide being silica or alumina) by the ALD technique. Commercial oxides, Grace 432 silica sieved to a particle size of 315–500  $\mu\text{m}$  and AKZO 001–1.5E alumina crushed and sieved to a particle size of 250–500  $\mu\text{m}$ , were used as supports. Prior to the ALD processing, the supports were heated in ambient air and further in vacuum to remove physisorbed water and to control the number of OH groups. The silica and alumina supports will be referred to in the form "750 °C oxide," where the temperature refers to the heat-treatment temperature. The characteristics of the supports are summarised in Table 3.1. According to nitrogen physisorption measurements, micropores were not present either in the silica or in the alumina support.

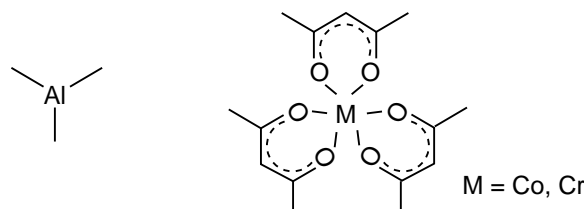
Aluminium nitride was prepared on silica and alumina by repeating the separate, saturating reactions of TMA and ammonia. Cobalt was deposited on silica and AlN/silica supports from  $\text{Co}(\text{acac})_3$  and chromium on alumina and AlN/alumina supports from  $\text{Cr}(\text{acac})_3$ . The structures of the metal reactants are shown in Figure 3.1, and the prepared samples are described in Table 3.2. The sample processing was done in an ALD reactor (ASM Microchemistry, Finland) operating in a vacuum of about 5 kPa. Typically, 5 to 10 g of support was used. The TMA, ammonia and oxygen reactants were introduced to the reactor by external syringes.  $\text{Co}(\text{acac})_3$ ,  $\text{Cr}(\text{acac})_3$  and water were placed in reactant vessels inside the ALD reactor where their evaporation temperature could be controlled.

**Table 3.1:** Characteristics of the silica and alumina supports.

Notation	Heat treatment:		Surface area $\text{m}^2 \text{g}^{-1}$	Pore volume $\text{cm}^3 \text{g}^{-1}$	OH groups per $\text{nm}^2$	Publication
	temperature, time					
	Ambient air	Vacuum				
200 °C silica	200 °C, 16 h	200 °C, 3 h	330	1.1	5.8	V
600 °C silica	600 °C, 16 h	450 °C, 3 h	330	1.1	1.6	V
750 °C silica	750 °C, 16 h	550 °C, 3 h	290	1.0	1.1	I, III–V
200 °C alumina	—	200 °C, 10 h	<sup>a</sup>	<sup>a</sup>	8.7	II, VII
400 °C alumina	—	400 °C, 10 h	255	0.64	6.0	II, VII
560 °C alumina	— <sup>b</sup>	560 °C, 10 h	<sup>a</sup>	<sup>a</sup>	2.0	II, VII
800 °C alumina	800 °C, 16 h	560 °C, 3 h	196	0.65	1.2	II, IV, VII

<sup>a</sup> Similar values as for 400 °C alumina (II). <sup>b</sup> Alternatively, the sample could be treated in air at 600 °C for 16 h and subsequently in vacuum at 560 °C for 3 h (II).

The reactants were led through the support bed, stabilised at the reaction temperature, in a stream of nitrogen. After each reaction, the support bed was purged with nitrogen at the reaction temperature. Thereafter, another saturating reaction was carried out, or the reactor was cooled close to room temperature and the samples were transferred inertly to a nitrogen-filled glove box.

**Figure 3.1:** Schematic representations of the structures of TMA,  $\text{Co}(\text{acac})_3$  and  $\text{Cr}(\text{acac})_3$ .

The samples surfaced with aluminium nitride will be referred to as " $n \cdot \text{AlN}/\text{oxide}$ ," where  $n$  denotes the number of times the reaction cycle of TMA and ammonia was repeated. The  $n \cdot \text{AlN}/\text{oxide}$  samples to be used as supports for cobalt and chromium catalysts were transferred back to the ALD reactor, where they were treated with ammonia at 550 °C to regenerate the surface, which inevitably had been slightly exposed to air during the transfer.

**Table 3.2:** Samples prepared by repeated separate, saturating gas–solid reactions (ALD technique).

Support	Reactions	Publications
750 °C silica	TMA at 150 °C	I
	TMA at 150 °C followed by ammonia at 150, 200, 250, 300, 350, 400, 450, 500 or 550 °C	I
	Ammonia at 550 °C followed by 3 × (TMA at 150 °C and ammonia at 400 °C)	III
	6 × (TMA at 150 °C and ammonia at 550 °C)	IV
200, 400, 560 and 800 °C alumina	TMA at 150 °C	II
560 °C alumina	TMA at 80, 150, 200, 250, 300, 327 and 350 °C	II
	TMA at 150 °C followed by ammonia at 150, 250, 350, 450 or 550 °C	II
800 °C alumina	6 × (TMA at 150 °C and ammonia at 550 °C)	IV
200, 600 and 750 °C silica, 2·AlN/silica, 6·AlN/silica	Co(acac) <sub>3</sub> at 180 °C	V, VI
200, 400, 560 and 800 °C alumina, 2·AlN/alumina, 6·AlN/alumina	Cr(acac) <sub>3</sub> at 200 °C	VII
800 °C alumina	Cr(acac) <sub>3</sub> at 200 °C and oxygen, water or ammonia at 550 °C	VII
2·AlN/alumina, 6·AlN/alumina	Cr(acac) <sub>3</sub> at 200 °C and ammonia at 550 °C	VII

## 3.2 Characterisation of samples

The samples were characterised by elemental analysis. The aluminium loading of the samples was measured with X-ray fluorescence spectroscopy (XRF) (I–IV), the carbon loading with a LECO analyser by burning at 950 °C in air (I–IV) or with a Ströhlein analyser by burning at 1350 °C in air (VI, VII), the nitrogen loadings with the LECO analyser (I–IV) and the cobalt and chromium loadings by atomic absorption spectroscopy (V–VII). The impurities present in the alumina support were measured semiquantitatively by XRF (II). The other characterisation techniques and their targets are listed in Table 3.3.

**Table 3.3:** Techniques used for the characterisation of the samples.

Technique	Target	Publications
N <sub>2</sub> -physisorption	Determination of specific surface area and pore volume	I, II, IV, V
Diffuse reflectance infrared Fourier transform (DRIFT) spectroscopy	Identification of adsorbed species	I–VII
Solid state nuclear magnetic resonance (NMR) spectroscopy		
a. <sup>1</sup> H magic-angle spinning (MAS) NMR	Identification and quantification of hydrogen-containing species	I, II, IV
b. <sup>13</sup> C cross-polarisation (CP) MAS NMR	Identification of carbon-containing species	I, II
c. <sup>27</sup> Al MAS NMR	Identification of aluminium species	III, IV
d. <sup>29</sup> Si CPMAS NMR	Identification of silicon-bonded species	I, III, IV
Scanning electron microscopy combined with energy-dispersive X-ray spectroscopy (SEM–EDS)	Determination of the distribution of aluminium in aluminium-nitride-modified silica	IV
Low-energy ion scattering (LEIS)	Determination of the relative composition of the outermost surface	IV
Thermogravimetry–differential thermal analysis (TG–DTA)	Identification of the evaporation temperature range suitable for Co(acac) <sub>3</sub>	V
H <sub>2</sub> -chemisorption	Evaluation of the surface area of metallic cobalt	VI
X-ray diffraction (XRD)	Identification of crystalline phases	IV
Electron spin resonance (ESR) spectroscopy	Identification of chromium species	VII

### 3.3 Evaluation of catalytic activity

The activity of cobalt catalysts prepared by ALD on silica and AlN/silica supports—750 °C silica, 2·AlN/silica and 6·AlN/silica—was evaluated in hydroformylation at 175 °C and 0.5 MPa (VI). A fixed-bed continuous flow reactor was used. The reaction

products were analysed by gas chromatography. The feed, total of  $7 \text{ dm}^3 \text{ h}^{-1}$ , consisted of argon, carbon monoxide, hydrogen and ethene in molar ratio 1:2:2:2, and it had an ethene weight hourly space velocity (WHSV) of  $2.5 \text{ h}^{-1}$ . Before the measurement, the catalysts were treated in situ with hydrogen at  $550 \text{ }^\circ\text{C}$ .

The activity of chromium catalysts prepared by ALD on alumina and AlN/alumina supports— $800 \text{ }^\circ\text{C}$  alumina, 2·AlN/alumina and 6·AlN/alumina—was evaluated in dehydrogenation at  $580 \text{ }^\circ\text{C}$  under atmospheric pressure (VII). Before the measurements, the catalysts prepared on  $800 \text{ }^\circ\text{C}$  alumina were activated by removing the acac ligands by treatment at  $550 \text{ }^\circ\text{C}$  with oxygen, water or ammonia. For catalysts prepared on the  $n$ ·AlN/alumina supports, ammonia was used for ligand removal because of the sensitivity of the supports to oxygen and water. A fixed-bed continuous flow reactor was used for the activity measurements. The reaction products were analysed with a Fourier transform infrared spectroscopy gas analyser and a gas chromatograph. Isobutane with a WHSV of  $15 \text{ h}^{-1}$ , diluted with nitrogen to a molar ratio of 3:7, was used as the feed. The catalysts deactivated during time on stream, and they were regenerated by air treatment. Three cycles of dehydrogenation and regeneration were carried out.

# Chapter 4

## Modification of porous oxides with aluminium nitride

Aluminium nitride was deposited on porous silica and alumina supports by repeating the separate, saturating reactions of TMA and ammonia (I–IV). Section 4.1 describes the reaction of TMA with the oxide supports (I, II). The surface reactions involved in the ALD growth of aluminium oxide thin films from TMA and water (II) are discussed as well, and a model is derived to relate the properties of the metal reactant to the amount of metal deposited in one ALD reaction cycle. Section 4.2 describes the reaction of ammonia with the TMA-modified supports (I, II). The growth of aluminium nitride in repeated reactions of TMA and ammonia is presented in Section 4.3 (III, IV). Finally, Section 4.4 highlights the special characteristics of the growth of aluminium nitride on porous oxide surfaces in a comparison with the growth of other materials by ALD.

### 4.1 Reaction of trimethylaluminium (TMA) with silica and alumina

The reaction of TMA was investigated at 150 °C with silica heat-treated at 750 °C (I) and at 80–350 °C with alumina heat-treated at 200–800 °C (II).

#### 4.1.1 Verification of surface saturation

To investigate whether the reaction of TMA at 150 °C with 750 °C silica is saturating, the aluminium concentrations in the top and bottom parts of the support bed were measured as a function of TMA dose (I). The aluminium concentrations increased with TMA dose

until they settled to a constant and similar value at top and bottom when the TMA dose was  $2.8 \text{ mmol g}_{\text{silica}}^{-1}$  or over (Figure 2, I). Thus, the TMA reaction with silica is saturating by nature. Homogeneous distribution of aluminium inside the silica particles was further confirmed by SEM–EDS measurements (Figure 7, IV).

Saturation was also concluded for the TMA reaction at 80–300 °C with alumina supports on the basis of the almost identical carbon contents in the top and bottom parts of the support bed (II). For reaction at 327 °C and above, the carbon content was higher in the top part of the alumina bed (II). The uneven carbon contents together with the darker sample colour and new features in DRIFT spectra indicated decomposition of TMA at 327 °C and above (II).

#### 4.1.2 Reaction with OH groups and oxygen bridges

The reaction of gaseous TMA with silica and alumina supports has been investigated by numerous groups.<sup>46,48,69,81–83,95,122–141</sup> TMA reacts with the hydrogen atoms in OH groups on oxide surfaces, producing O–Al bonds and releasing methane (4.1).<sup>46,48,81,82,125,132–134,136</sup>



The TMA reaction caused the disappearance of features attributable to OH groups and the simultaneous appearance of features of aluminium-bonded methyl groups (Al–Me) in DRIFT, <sup>1</sup>H MAS NMR and <sup>13</sup>C CPMAS NMR spectra (I–III).

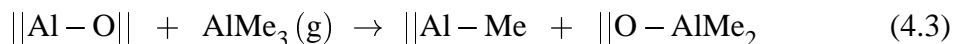
In addition to the ligand exchange reaction (4.1), TMA reacts dissociatively with the siloxane bridges of silica (4.2).<sup>81–83,125,126,142</sup>



In this reaction, silicon-bonded methyl groups are formed, as evidenced by DRIFT, <sup>1</sup>H MAS NMR, <sup>13</sup>C CPMAS NMR and <sup>29</sup>Si CPMAS NMR investigations (I, III, IV).

A possible dissociative reaction of TMA with the c.u.s. Al–O pairs of alumina has also been discussed in the literature. Dillon et al.<sup>136</sup> propose that this type of reaction could take place, but Ott et al.<sup>69</sup> and Juppo et al.<sup>138</sup> report that it would play only a minor role when aluminium oxide thin films are grown by ALD from TMA and water. To clarify the occurrence of a possible dissociative reaction in c.u.s. Al–O pairs, the reaction of TMA was investigated on highly dehydroxylated alumina samples (II). The amount of TMA chemisorbed on alumina dehydroxylated at 560 °C and 800 °C exceeded the maximum possible amount calculated by assuming that OH groups are the only reactive sites (Figure 12, II). Thus, there must be an alternative path for chemisorption of TMA

on alumina. The dissociative reaction to Al–O pairs (4.3) seems to be the most likely alternative.



The OAlMe<sub>2</sub> species that are initially produced in reactions 4.1–4.3 have been suggested to react further with neighbouring hydrogen atoms in OH groups and with siloxane bridges, to form O<sub>2</sub>AlMe species<sup>82,136,137</sup> or even O<sub>3</sub>Al species.<sup>136,137</sup> The results obtained in this work confirmed that further reaction takes place: according to <sup>13</sup>C CPMAS NMR measurements, after the TMA reaction at 150 °C on silica heat-treated at 750 °C, there were on average 1.4 methyl groups bonded to each aluminium atom (I). Bartram et al.<sup>82</sup> further suggested that the reaction would always proceed to O<sub>2</sub>AlMe species; however, the <sup>13</sup>C CPMAS NMR results of this work (I) do not support their suggestion.

On the silica surface, in addition to the various OAlMe<sub>2</sub>, O<sub>2</sub>AlMe and O<sub>3</sub>Al species, various species containing Si–Me groups are formed. Lakomaa et al.<sup>83</sup> showed by <sup>29</sup>Si CPMAS NMR measurements that O<sub>3</sub>SiMe, O<sub>2</sub>SiMe<sub>2</sub> and OSiMe<sub>3</sub> species are formed in the reaction. These same O<sub>4–m</sub>SiMe<sub>m</sub> species (*m* = 1, 2 or 3) were observed by <sup>29</sup>Si CPMAS NMR in this work (I). More O<sub>4–m</sub>SiMe<sub>m</sub> species form the higher the silica heat-treatment temperature and the TMA reaction temperature.<sup>83</sup> Their extensive formation was avoided here by use of a rather low reaction temperature, 150 °C.

### 4.1.3 Factor determining the surface saturation

The saturating reaction of TMA was investigated quantitatively at various temperatures with supports differing substantially in their nature and number of reactive sites. The TMA reaction at 150 °C was investigated on silica heat-treated at 750 °C that contained OH groups and siloxane bridges (I); on ammonia-modified silica that contained NH<sub>2</sub> groups, OH groups and siloxane bridges (III); on alumina heat-treated at 200–800 °C that contained various numbers of OH groups and c.u.s. Al–O pairs (II); and on aluminium nitride surfaced silica and alumina that contained NH<sub>x</sub> groups and oxygen and nitrogen bridges (IV). Furthermore, the saturating reaction of TMA was investigated at 80–300 °C on alumina heat-treated at 560 °C (II). In all cases, the methyl group content (i.e., the carbon content) settled to 5–6 Me nm<sup>–2</sup> (I–IV). This methyl group content is in accord with that found by Anwander et al.<sup>137</sup> for TMA-modified MCM-41 silicate (4.8 Me nm<sup>–2</sup>) and by Uusitalo et al.<sup>95</sup> for TMA-modified silica (5.7–6.1 Me nm<sup>–2</sup>).

Obtaining the same result for a wide variety of supports and reaction temperatures indicates that the achievement of surface saturation is defined by the steric hindrance imposed by the methyl ligands, regardless of the reactive sites on the support. Further

support for this interpretation is obtained by comparing the achieved methyl group content with the theoretical highest possible content (I). For methyl groups with a van der Waals radius of  $0.20 \text{ nm}^{143}$  and hexagonal packing, the maximum possible content is  $7.2 \text{ Me nm}^{-2}$  (I). The observed methyl group content is about 70–80% of this upper limit, supporting the idea that the chemisorption of TMA proceeds as long as sufficiently large areas not blocked by the methyl ligands remain on the surface (I).

It is now known that (i) the methyl group content settles to a constant value when surface saturation is attained and (ii) (practically) all hydrogen atoms in OH groups are consumed in the TMA reaction and released as methane. Since the Me/Al ratio in the TMA molecule is three, the amount of aluminium attached to the surface in the TMA reaction,  $\Delta c_{\text{Al}}$  [ $\text{at}_{\text{Al}} \text{ nm}^{-2}$ ], can be calculated from the elemental balance (4.4) (I,II):

$$\Delta c_{\text{Al}} = \frac{1}{3} \left( \Delta c_{\text{Me}} + \Delta c_{(\text{O})\text{H}} \right), \quad (4.4)$$

where  $\Delta c_{\text{Me}}$  is the amount of methyl groups after the chemisorption and can be taken as  $5 \text{ Me nm}^{-2}$  (see above), and  $\Delta c_{(\text{O})\text{H}}$  is the amount of hydrogen atoms reacted [ $\text{at}_{\text{H}} \text{ nm}^{-2}$ ], which can be approximated with the total amount of hydrogen atoms in surface OH groups,  $c_{(\text{O})\text{H}}$  [ $\text{at}_{\text{H}} \text{ nm}^{-2}$ ] (I,II). The amounts of aluminium attached in the TMA reaction to various silica and alumina supports, calculated from equation 4.4, are shown in Figure 4.1. The equilibrium OH group contents (see Section 2.1.2, p. 17) are included for reference. In the case of silica, the calculated aluminium contents are in excellent agreement with the contents measured in this work (I) and by Uusitalo et al.<sup>95</sup> The results of Lakomaa et al.<sup>83</sup> deviate from the trend of Figure 4.1, however, perhaps because of partial oxidation of TMA to form methoxy groups. The agreement on silica and the similar reaction mechanisms on silica and alumina suggest that the calculated contents also should be reliable for alumina.

#### 4.1.4 Growth of aluminium oxide from TMA and water by ALD

The results obtained for the TMA reaction on porous oxides can be compared with the results obtained for the same reaction in ALD growth of aluminium oxide thin films from TMA and water. The average increase in film thickness per cycle,  $\Delta h_{\text{AlO}_{1.5}}$  [ $\text{nm}(\text{cycle})^{-1}$ ], is directly related to the amount of aluminium deposited per cycle,  $\Delta c_{\text{Al}}$  [ $\text{at}_{\text{Al}} \text{ nm}^{-2}$ ]. The atomic density of aluminium oxide,  $v_{\text{AlO}_{1.5}}$  [ $\text{nm}^{-3}$ ], is:

$$v_{\text{AlO}_{1.5}} = \frac{\rho_{\text{AlO}_{1.5}} N_{\text{A}}}{M_{\text{AlO}_{1.5}}}, \quad (4.5)$$

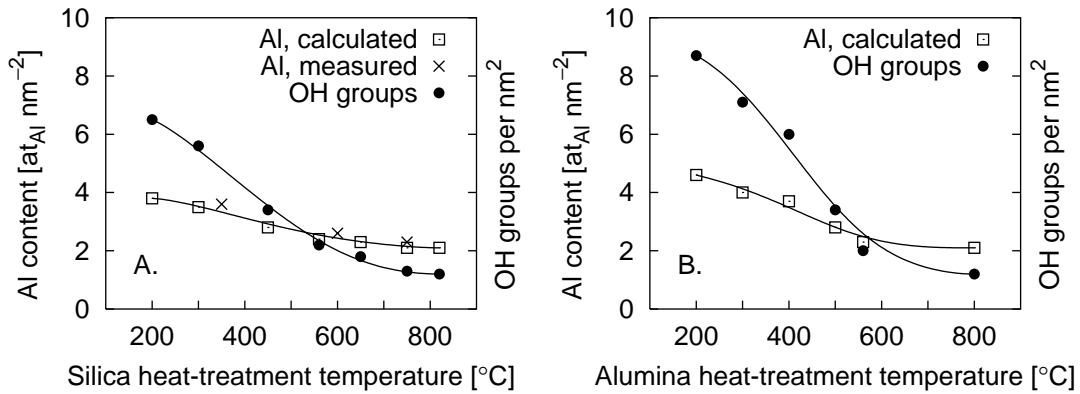


**Figure 4.1:** Amounts of aluminium attached on (A) silica and (B) alumina, calculated from equation 4.4 using the equilibrium OH group contents of silica<sup>77</sup> and alumina (II) and assuming a methyl group content of 5 Me nm<sup>-2</sup>. Aluminium contents measured after the saturating reaction of TMA with 350 and 600 °C silica<sup>95</sup> and with 750 °C silica (I) and the equilibrium OH group contents on silica<sup>77</sup> and alumina (II) are also shown.

where  $\rho_{\text{AlO}_{1.5}}$  is the density of aluminium oxide [ $\text{g nm}^{-3}$ ], and the amount of aluminium deposited per cycle is:

$$\Delta c_{\text{Al}} = v_{\text{AlO}_{1.5}} \Delta h_{\text{AlO}_{1.5}} \quad (4.6)$$

$$= \frac{\rho_{\text{AlO}_{1.5}} N_{\text{A}}}{M_{\text{AlO}_{1.5}}} \Delta h_{\text{AlO}_{1.5}} \quad (4.7)$$

Figure 4.2 shows the amount of aluminium deposited in one reaction cycle (i.e., in the TMA reaction), according to the results of Ott et al.,<sup>69</sup> calculated by equation 4.7 with  $\rho_{\text{AlO}_{1.5}}$  of  $3.5 \times 10^{-21} \text{ g nm}^{-3}$ . When the reaction of water on the TMA-modified surface is saturated, the surface OH group content on the grown aluminium oxide film should be the equilibrium OH group content at the applied reaction temperature. Thus, the amount of aluminium deposited in the TMA reaction in thin film growth should be the same as the amount of aluminium deposited in the TMA reaction on porous alumina with corresponding OH group content. Figure 4.2 also shows the amount of aluminium calculated to be deposited on alumina that has the equilibrium OH group content typical for heat-treatment at 200–300 °C (for calculations, see explanations to Figure 4.1). Evidently, quantitative results obtained for the TMA reaction in thin film growth<sup>69</sup> and on porous materials (II) agree.

The growth of aluminium oxide thin films from TMA and water was recently investigated by Juppo et al. and Rahtu et al. by in situ mass spectrometry<sup>138–141</sup> and quartz crystal microbalance measurements.<sup>140,141</sup> In their investigations, the growth was described

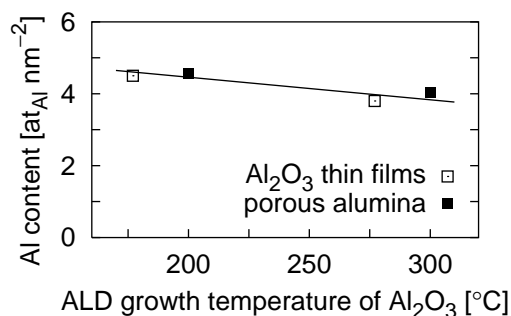
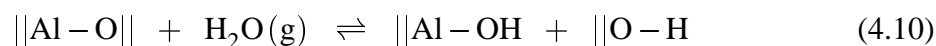
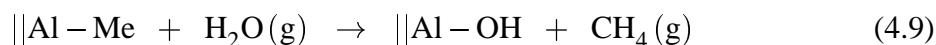


**Figure 4.2:** The amount of aluminium atoms attached per square nanometre of surface in one reaction cycle of TMA and water in ALD growth of aluminium oxide, calculated from the results obtained for thin film growth<sup>69</sup> and for porous alumina (II).

through ligand exchange reactions of TMA (4.8) and water (4.9) and the dissociative reaction of water (4.10).



As shown by Rahtu et al.,<sup>140,141</sup> the results of Juppo et al.<sup>138,139</sup> represent conditions where ligand exchange reactions (4.8,4.9), which produce gaseous reaction products, had saturated, but the dissociative reaction of water (4.10) had not. This means that the OH group content on the water-treated surface was less than the equilibrium OH group content, and c.u.s Al-O sites were exposed on the surface. Information on the reaction mechanisms of TMA can be acquired by examining the results of Juppo et al.<sup>138,139</sup> more closely. The amount of methyl groups remaining after the TMA reaction increased sharply with reaction temperature (Figure 5A in Ref. 138). Because elevated temperature accelerates reactions, under unsaturated conditions the amount of reaction products can be expected to increase with reaction temperature. Since the methyl group content settles to the same value at saturation irrespective of temperature (see Section 4.1.3, p. 32) and the methyl group content did not reach a constant value, the dissociation of TMA in c.u.s. Al-O pairs (4.3) must not have reached saturation level in their experiments. The results of Juppo et al.<sup>138,139</sup> thus provide further experimental evidence that TMA reacts dissociatively with the c.u.s. Al-O sites.

As a conclusion, there is quantitative agreement between the results obtained for TMA reaction in ALD thin film growth and on porous materials. This appears to be the first time that such an agreement has been demonstrated. Where differences in the TMA reaction have been seen, they have resulted from use of unsaturated reactions in thin film growth,

not from differences in the types of reactions taking place on supports characterised by different dimensions.

#### 4.1.5 Summary of the TMA reaction

The reaction of TMA is saturating on silica and alumina at least from room temperature up to about 300 °C. Two types of reactions take place on these supports: ligand exchange reaction with OH groups (4.1) and dissociation in oxygen bridges (4.2, 4.3). Most likely, the silica and alumina materials can be taken to represent a larger group of oxide materials, and the saturating reaction of TMA with oxide surfaces can be summarised as follows:

1. TMA reacts with practically all hydrogen atoms in OH groups, releasing methane and attaching to the surface as an  $\text{AlMe}_n$  complex ( $n = 0, 1, 2$ ).
2. TMA (or surface  $\text{AlMe}_n$ ) reacts dissociatively with oxygen bridges, with all methyl groups bonded to the surface.
3. The endpoint of the reaction and saturation of the surface with adsorbed species is achieved when the methyl group content is  $5\text{--}6 \text{ Me nm}^{-2}$ .

From points 1, 2 and 3 it is clear that the Me/Al ratio on the surface depends on the amount of hydrogen atoms in OH groups on the starting surface, according to:

$$\text{Me/Al} = 3 \left( 1 + \frac{c_{(\text{O})\text{H}}}{\Delta c_{\text{Me}}} \right)^{-1}. \quad (4.11)$$

#### 4.1.6 Relation of size and reactivity of $\text{ML}_n$ reactant to ALD growth of $\text{MO}_x$ material

The agreement between the results obtained for the TMA reaction on porous materials and in thin film growth encouraged the derivation of an expression that relates the size of a metal reactant  $\text{ML}_n$  and its reactivity with oxide materials to the growth of  $\text{MO}_x$  material in one ALD reaction cycle ( $\text{at}_{\text{M}} \text{ nm}^{-2} (\text{cycle})^{-1}$  or  $\text{nm} (\text{cycle})^{-1}$ ).<sup>144</sup>

In the growth by ALD from  $\text{ML}_n$  and water, according to mass balance, the amount of ligands attached to the surface in one saturating  $\text{ML}_n$  reaction,  $\Delta c_{\text{L}}$  [ $\text{L nm}^{-2}$ ], is proportional to (i) the amount of metal attached,  $\Delta c_{\text{M}}$  [ $\text{at}_{\text{M}} \text{ nm}^{-2}$ ], and (ii) the amount ligands released in the ligand exchange reaction with (O)H groups, that is, the number of reacted (O)H groups,  $\Delta c_{(\text{O})\text{H}}$  [ $\text{at}_{\text{H}} \text{ nm}^{-2}$ ]:

$$\Delta c_{\text{L}} = n \Delta c_{\text{M}} - \Delta c_{(\text{O})\text{H}}. \quad (4.12)$$

The amount of metal M attached to the surface in one saturating  $ML_n$  reaction is, accordingly:

$$\Delta c_M = \frac{1}{n} (\Delta c_L + \Delta c_{(O)H}). \quad (4.13)$$

A requirement for maximum ALD growth per cycle is that the reaction proceeds as long as there is space for  $ML_n$  to interact with the surface; that is, saturation is defined by the steric hindrance imposed by the ligands. The coverage of ligands at saturation,  $\theta$ , is defined as:

$$\theta = \frac{\Delta c_L}{\Delta c_L^{\text{maxtheor}}}, \quad (4.14)$$

where  $\Delta c_L^{\text{maxtheor}}$  [ $L \text{ nm}^{-2}$ ] denotes the theoretical upper limit of  $\Delta c_L$  and is obtained from the filling area of the ligands,  $a_L$  [ $\text{nm}^{-2}$ ]:

$$\Delta c_L^{\text{maxtheor}} = \frac{1}{a_L}. \quad (4.15)$$

For spherical ligands,  $a_L$  can be calculated, as illustrated in Figure 4.3, by assuming hexagonal packing of the ligands and a radius of  $r_L$  [nm]:

$$a_L = 2\sqrt{3}r_L^2. \quad (4.16)$$

In practice,  $\theta$  of one is not reached, because of the larger size of the  $ML_n$  molecule than a single ligand and because the reactive sites on the surface may be located so that they do not allow very tight packing.

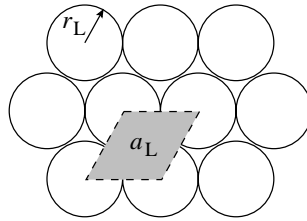


**Figure 4.3:** Filling area  $a_L$  of ligand L with radius  $r_L$  for hexagonal packing.

To relate the amount of hydrogen atoms reacted,  $\Delta c_{(O)H}$ , to the amount of hydrogen atoms in OH groups on the surface after the reaction of water,  $c_{(O)H}$  [ $\text{at}_H \text{ nm}^{-2}$ ], the fraction of hydrogen atoms reacted with  $ML_n$ ,  $f$ , is introduced:

$$f = \frac{\Delta c_{(O)H}}{c_{(O)H}}. \quad (4.17)$$

In the ideal case,  $f$  is one.

Combining equations 4.13, 4.14 and 4.17, we get an expression that relates the amount of metal deposited to the size of the  $ML_n$  reactant ( $n$ ,  $\Delta c_L^{\text{maxtheor}}$ ) and its reactivity with oxide materials ( $\theta$ ,  $f$ ):

$$\Delta c_M = \frac{1}{n} \left( \theta \Delta c_L^{\text{maxtheor}} + f c_{(\text{O})\text{H}} \right). \quad (4.18)$$

The increase in film thickness in one reaction cycle of ALD thin film growth,  $\Delta h_{\text{MO}_x}$  [ $\text{nm}(\text{cycle})^{-1}$ ], is related to the amount of metal deposited in one reaction cycle through the following formula (derivation in Section 4.1.4, p. 33):

$$\Delta h_{\text{MO}_x} = \frac{M_{\text{MO}_x}}{\rho_{\text{MO}_x} N_A} \Delta c_M. \quad (4.19)$$

Because the ALD technique is based on the systematic employment of surface saturation, the amount of hydrogen atoms in OH groups present before the reaction of  $ML_n$  should equal the amount of hydrogen atoms in OH groups at equilibrium at the growth temperature on the  $\text{MO}_x$  material,  $c_{(\text{O})\text{H}}^{\text{eq}}$  [ $\text{at}_\text{H} \text{nm}^{-2}$ ]:

$$c_{(\text{O})\text{H}} = c_{(\text{O})\text{H}}^{\text{eq}}. \quad (4.20)$$

Combining equations 4.18, 4.19 and 4.17, we obtain an expression that relates the increase in film thickness per cycle to the properties of the  $ML_n$  reactant ( $n$ ,  $\Delta c_L^{\text{maxtheor}}$ ,  $\theta$ ,  $f$ ) and the  $\text{MO}_x$  material ( $c_{(\text{O})\text{H}}^{\text{eq}}$ ):

$$\Delta h_{\text{MO}_x} = \frac{M_{\text{MO}_x}}{\rho_{\text{MO}_x} N_A n} \left( \theta \Delta c_L^{\text{maxtheor}} + f c_{(\text{O})\text{H}}^{\text{eq}} \right). \quad (4.21)$$

The maximum growth per cycle is obtained when (i) the reaction proceeds until all available space on the surface has been consumed, that is,  $\theta$  is maximum, and (ii) all hydrogen atoms in OH groups react, that is,  $f$  is one. For TMA, maximum  $\theta$  was identified as about 0.7. In the absence of experimental values, this value probably provides a useful estimate for other reactants with similar reactivities. Greater increase in film thickness per cycle than given by equation 4.21 with  $\theta = 1$  and  $f = 1$  means that growth does not take place purely in ALD mode. Instead, the reactions are not saturating, CVD-type growth occurs, or physisorption or decomposition takes place. Less growth per cycle than given by equation 4.21 with  $\theta \approx 0.7$  and  $f = 1$  may indicate that:

1. The reaction stops without achieving a dense ligand packing. This corresponds to small  $\theta$  and indicates that the  $ML_n$  reactant has a low reactivity; for example, no dissociative reaction takes place.

2. The  $ML_n$  reactant does not react with all OH groups on the surface. This corresponds to  $f$  of below one. The  $ML_n$  reactant may react selectively with certain types of OH groups, for example, isolated OH groups.
3. The gaseous reaction products, LH, released in the ligand exchange reaction of  $ML_n$  with OH groups, readsorb on the surface. This corresponds to case where no (or few) ligands are released through reaction with OH groups, and  $f$  is zero (or low).

A model comparable to that derived here has been presented by Ylilammi.<sup>145</sup> His model relates the ALD thin film growth to packing density,  $p$ , and the lattice constant,  $a$ , of anions of material  $BA_x$  ( $A$  = anion) arranged in a square surface lattice. The packing density is obtained by assuming a certain geometry for the adsorbed species, that is, a certain L/M ratio, and calculating the size of the adsorbed complex. In the model of Ylilammi, the L/M ratio is assumed to have an integer value, whereas in the present model also non-integer values are acceptable, as the L/M ratio is obtained from:

$$L/M = n \left( 1 + \frac{f c_{(OH)}^{eq}}{\theta \Delta c_L^{maxtheor}} \right)^{-1}. \quad (4.22)$$

Because Ylilammi's model<sup>145</sup> does not consider the surface reactions that take place, most importantly not the ligand exchange reaction that releases ligands from the surface, his model cannot account for growth that decreases steadily with increasing ALD growth temperature. In the case of the model presented here, the decrease in growth with increasing reaction temperature is inherent in the inclusion of ligand exchange reaction ( $f > 0$ ), as  $c_{(OH)}^{eq}$  typically decreases with increasing temperature. Also the maximum expected thin film growth differs in Ylilammi's model and the present model. For example, for the growth of aluminium oxide from TMA and water at 200 °C, where the Me/Al ratio is about one (see Figure 4.1, p. 34), Ylilammi's model would result in a maximum growth of  $0.075 \text{ nm}(\text{cycle})^{-1}$  [ $\rho_{AlO_{1.5}} = 3.5 \times 10^{-21} \text{ g nm}^{-3}$ ,  $a = 0.28 \text{ nm}$ ,  $d = 0.40 \text{ nm}$  (from the van der Waals radius of  $0.20 \text{ nm}$ <sup>143</sup>) and  $p = 1/4$ ].<sup>145</sup> The observed growth, about  $0.11 \text{ nm}(\text{cycle})^{-1}$ ,<sup>69</sup> is almost 50% higher than the maximum allowed by the model of Ylilammi. The present model, in turn, with parameters  $\theta = 0.7$  and  $f = 1$ , accounts for the growth of  $0.11 \text{ nm}(\text{cycle})^{-1}$  at 200 °C.

## 4.2 Reaction of ammonia with TMA-modified silica and alumina

The reaction of ammonia with TMA-modified silica and alumina was investigated at 150–550 °C (I,II). Elemental analysis indicated saturation of the surface with adsorbed species in both cases (I,II).

TMA-modified silica and alumina both contain aluminium-bonded methyl groups. In addition, TMA-modified silica contains silicon-bonded methyl groups. Aluminium-bonded methyl groups react with ammonia, releasing methane and generating aluminium-bonded NH<sub>2</sub> groups (4.23).<sup>44–47,49,52</sup>



Silicon-bonded methyl groups have been suggested not to react with ammonia.<sup>45</sup>

Comparison of the results obtained for TMA-modified silica and alumina is facilitated by expressing the results of carbon and nitrogen determinations as a function of ammonia reaction temperature, as shown in Figure 4.4. The amount of carbon present decreased with increasing reaction temperature on both supports. However, on silica, some carbon remained even after reaction at 550 °C, whereas on alumina the carbon content decreased below detection level in the reaction at 300 °C. On both supports the nitrogen content increased with ammonia reaction temperature up to about 300 °C; thereafter it remained at about constant level for silica but decreased for alumina.

DRIFT spectra recorded for TMA-modified silica (I) and alumina (II) after the ammonia reaction are shown together in Figure 4.5. The DRIFT results are in accord with

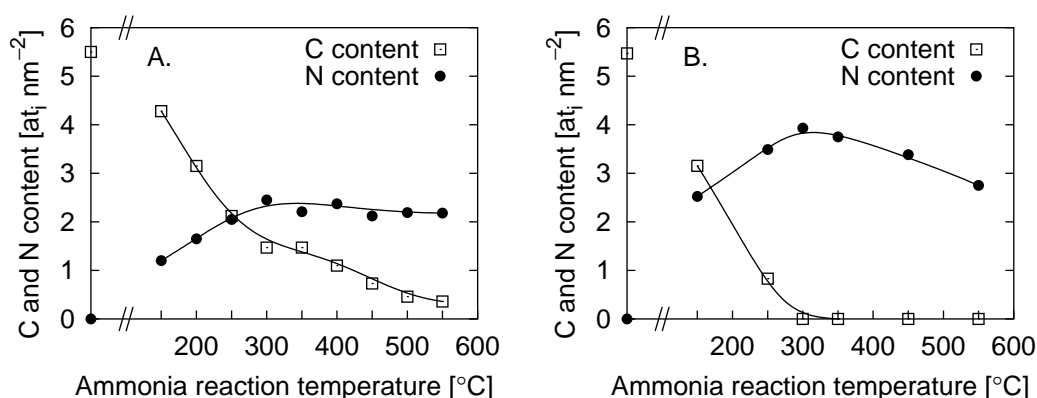


**Figure 4.4:** Average amounts of carbon and nitrogen present on (A) 750°C silica and (B) 560 °C alumina after TMA modification at 150 °C and subsequent ammonia reaction (I,II). Marks on the y-axis indicate the amounts before the ammonia reaction.

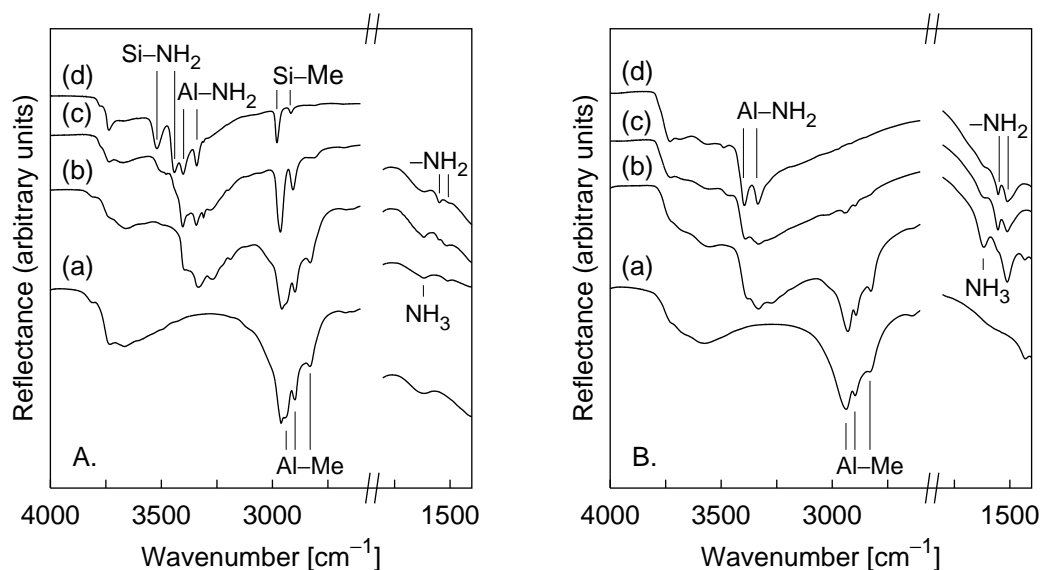


**Figure 4.5:** DRIFT spectra measured for (A) 750 °C silica and (B) 560 °C alumina after (a) TMA reaction at 150 °C, and successive ammonia reaction (b) at 150 °C, (c) at 350 °C and (d) at 550 °C (I,II).

the results of elemental analysis: only negligible features of methyl groups remain after ammonia reaction at 350 °C and above in the spectra of the samples prepared on alumina, whereas some peaks of methyl groups remain in the spectra of the samples prepared on silica. Only aluminium-bonded  $\text{NH}_x$  groups are observed in the spectra of the alumina samples, whereas both aluminium-bonded and silicon-bonded  $\text{NH}_x$  groups are present in the spectra of the silica samples (I,II). The appearance of  $\text{Si-NH}_x$  groups on silica and the decreased intensity of the  $\text{Si-Me}$  groups suggests that ammonia had partly reacted with the  $\text{Si-Me}$  groups, contrary to the suggestion of Bartram et al.<sup>45</sup> The  $^{29}\text{Si}$  CPMAS NMR and  $^{13}\text{C}$  CPMAS NMR measurements confirmed that 80% of the silicon-bonded methyl groups had been removed by ammonia (I).

The H/N ratio in the  $\text{NH}_x$  groups is of interest for estimating the types of amino groups formed on the surface. The total amount of hydrogen atoms in  $\text{NH}_x$  groups, in turn, is important in regard to eventual applications of the aluminium nitride surfaced supports. Average H/N ratios and the total amounts of hydrogen atoms in  $\text{NH}_x$  groups were calculated on the basis of an elemental balance, assuming that hydrogen was lost from the ammonia molecule or surface  $\text{NH}_x$  groups through reaction with methyl groups and release of methane (I,II). The calculated amounts and the amounts determined by  $^1\text{H}$  MAS NMR agreed (I,II). To facilitate comparison, the results for the silica and alumina supports are shown together in Figure 4.6. The trend in the H/N ratio is similar for the

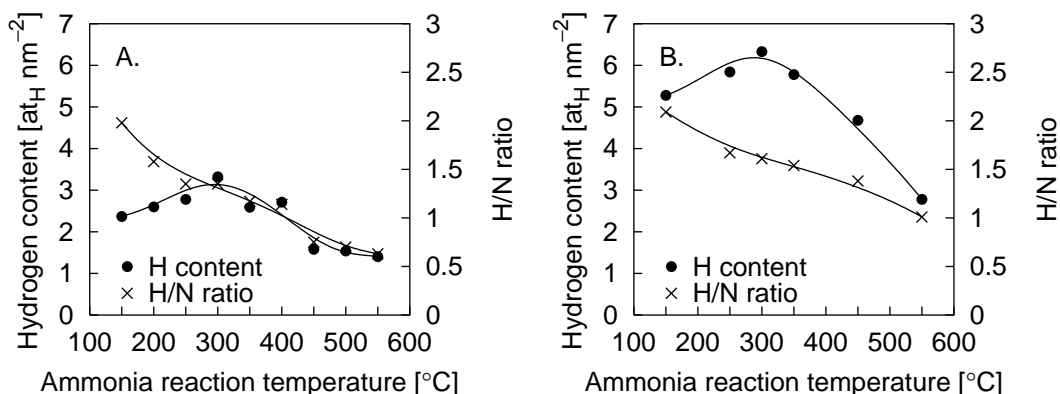
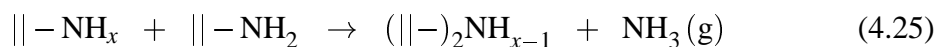
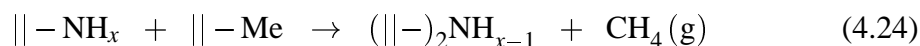


**Figure 4.6:** Total amount of hydrogen atoms present in  $\text{NH}_x$  groups (calculated from elemental analysis) and the average H/N ratio for TMA-modified supports subsequently reacted with ammonia: (A) 750 °C silica and (B) 560 °C alumina (I, II).

two supports: for reaction at 150 °C, the ratio is about two, and it decreases with increasing ammonia reaction temperature down to about one for ammonia reaction at 550 °C. However, the total hydrogen content is considerably higher for the alumina support at all reaction temperatures. The higher hydrogen content is mostly explained by the higher content of methyl groups removed and thus higher content of  $\text{NH}_x$  groups attached on alumina at all temperatures.

The decrease in the average H/N ratio in  $\text{NH}_x$  groups below two at reaction temperatures above 150 °C indicates either that the amino groups can react further with neighbouring methyl groups, releasing more methane (4.24), or that they can react with neighbouring secondary amino groups to release ammonia (4.25).



In the case of the alumina support, the average H/N ratio decreased even when ammonia reaction temperature was above 300 °C, when only negligible amounts of methyl groups were left on the support (see Figure 4.4). This indicates that reaction 4.25 took place. Such direct evidence does not exist for reaction 4.24.

On the basis of the average H/N ratios and the results of DRIFT,  $^1\text{H}$  MAS NMR and  $^{29}\text{Si}$  CPMAS NMR spectroscopy, a general picture was constructed of the surface species present on the TMA-modified supports after the reaction of ammonia at various temperatures (I, II). The structures are summarised in Figure 4.7.



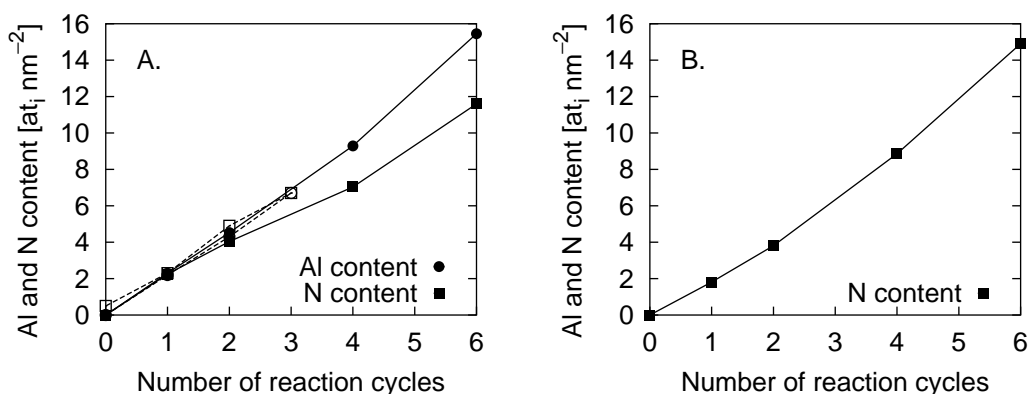


**Figure 4.8:** Aluminium and nitrogen contents measured for (A) 750 °C silica support and (B) 800 °C alumina support after repeated separate, saturating reactions of TMA and ammonia at 150 °C and 550 °C (IV), respectively. Open symbols connected by dashed lines show the results on silica for ammonia reaction at 400 °C (III).

reactions such as 4.24 and 4.25 also occurred, since the amount of nitrogen deposited per cycle was about half of the amount of methyl groups present after the TMA reaction.

The types of aluminium species present in the aluminium nitride surfaced samples were investigated by <sup>27</sup>Al MAS NMR (III, IV). After four reaction cycles of TMA and ammonia, Al–NH<sub>x</sub> species were identified in the <sup>27</sup>Al MAS NMR spectra for both AlN/silica and AlN/alumina (IV). Furthermore, after six reaction cycles, AlN<sub>4</sub> units were identified in the <sup>27</sup>Al MAS NMR spectra of AlN/alumina (IV). The aluminium nitride appeared amorphous in XRD, however (IV). According to surface area measurements, blocking of the pores of the supports by aluminium nitride species did not take place (IV).

The amount of hydrogen present in the NH<sub>x</sub> groups was determined for the AlN/silica and the AlN/alumina samples by <sup>1</sup>H MAS NMR (IV). As shown in Figure 4.9, the amount of hydrogen in NH<sub>x</sub> groups increased with the number of reaction cycles. Simultaneously, the average H/N ratio (i.e., average *x* in NH<sub>x</sub>) decreased. The increasing hydrogen content explains the slight increase in growth per cycle with number of reaction cycles (see Figure 9, IV), as more methyl groups were released in the ligand exchange reaction with TMA (reaction of type 4.1). Apparently, the maximum hydrogen content that can prevail on the AlN/oxide samples had not been reached after six reaction cycles, and the hydrogen content would increase with further cycles until it stabilised at some level.

The hydrogen atoms in NH<sub>x</sub> groups present on AlN/oxide surfaces can potentially serve as anchoring sites in the preparation of catalysts. They may also be sensitive to hydrolysis, however, which could destroy the nitride structure (IV).<sup>52</sup>

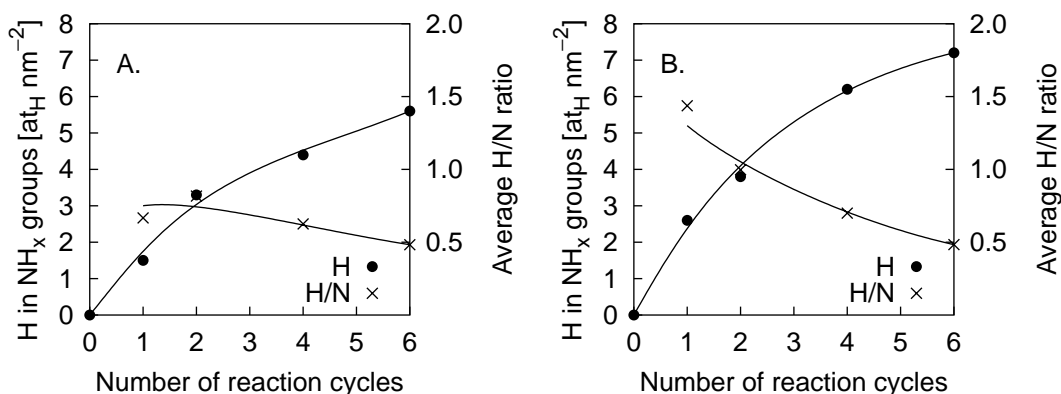


**Figure 4.9:** Amount of hydrogen present in NH<sub>x</sub> groups and the average H/N ratios on (A) AlN/silica samples and (B) AlN/alumina samples, as determined by <sup>1</sup>H MAS NMR (IV).

### 4.3.2 Coverage of silica with aluminium nitride

The coverage of silica by aluminium nitride was investigated by low energy ion scattering (LEIS) (IV). LEIS probes the elements present on the outermost surface of a material.<sup>146</sup> Although hydrogen atoms are not detected by LEIS, they shield other surface atoms and prevent them from being detected. This interference was avoided by cleaning the samples with atomic oxygen before recording of the LEIS spectra. The aluminium nitride species were oxidised in this treatment.

LEIS spectra measured for the AlN/silica samples are shown in Figure 4.10. The peak of oxygen is seen at constant energy in all spectra. The peak originating from aluminium and silicon atoms shifts to lower energy with increasing aluminium content, that is, closer to the energy of aluminium alone. A magnification of the Al–Si peak region of the spectra is presented in Figure 8A of Publication IV.

The coverage of silica by aluminium nitride was investigated by fitting individual Si and Al peaks to the combined Al–Si peak and determining the normalised peak intensities (IV). The results of the fitting are shown in Figure 4.11A. The coverage of silica by aluminium nitride increased gradually with the aluminium loading.

The trend in the coverage of silica by aluminium nitride with increasing aluminium loading carries information on the reaction mechanism of TMA with the surface species. Figure 4.12 illustrates three possibilities for the TMA reaction with increasing extent of aluminium nitride modification: (a) TMA reacts preferentially with silica, (b) TMA reacts with equal probability with silica and aluminium nitride species and (c) TMA reacts preferentially with aluminium nitride species. Curves (a), (b) and (c) in Figure 4.11B show the trends in coverage of silica by aluminium nitride that these reaction mechanisms

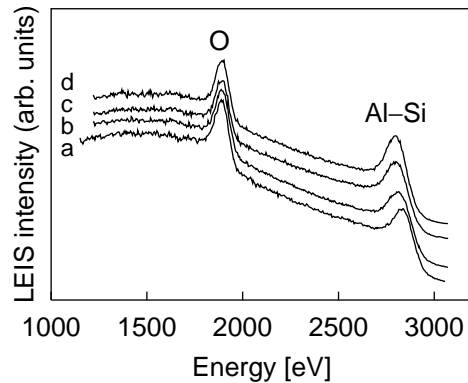


**Figure 4.10:** LEIS spectra for samples treated with atomic oxygen, measured by  $5 \text{ keV}^4\text{He}^+$  ions: (a) silica, (b)  $2 \cdot \text{AlN}/\text{silica}$ , (c)  $4 \cdot \text{AlN}/\text{silica}$  and (d)  $6 \cdot \text{AlN}/\text{silica}$ .

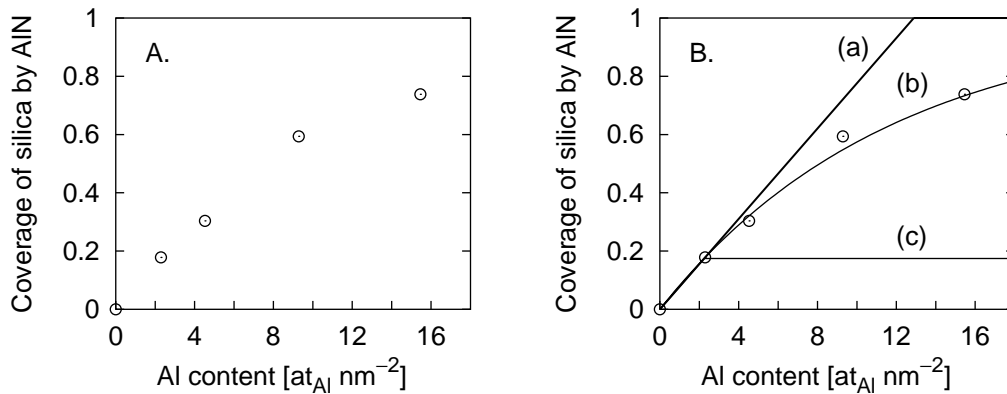


**Figure 4.11:** (A) Coverage of silica by aluminium nitride as determined by LEIS (IV). (B) Trend in the coverage of silica by aluminium nitride when mechanisms (a), (b) and (c) of Figure 4.12 are operative. The experimental point at  $x = 2.297 \text{ at}_{\text{Al}} \text{ nm}^{-2}$  and  $y = 0.1782$  defines curve (b):  $y = 1 - (1 - 0.1782)^{(x/2.297)} = 1 - e^{-0.08544x}$ .

would lead to. Model (b) is in full agreement with the LEIS results. Thus, TMA appears to react with equal probability with all the surface sites: OH groups,  $\text{NH}_x$  groups, oxygen bridges and nitrogen bridges (IV).

## 4.4 Comparison of ALD growth of aluminium nitride with growth of other materials

In the growth of aluminium nitride from TMA and ammonia, the amount of aluminium deposited per cycle increased slightly with the number of reaction cycles (Figure 4.8).

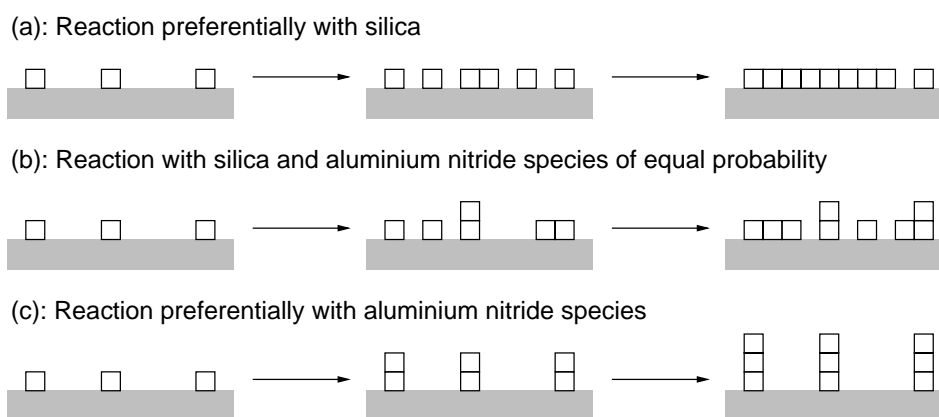


**Figure 4.12:** Schematic illustration showing how preferential chemisorption of TMA would affect the increase in coverage with increasing amount of deposited material.

This was due to the increasing amount of hydrogen on the surface (Figure 4.9). An increasing trend has not been observed for other ALD processes investigated on porous materials.

A larger amount of metal was deposited per cycle in the growth of aluminium nitride than in the growth of other materials prepared on porous supports. In the TMA–ammonia process, about  $2.4 \text{ at}_{\text{Al}} \text{ nm}^{-2}$  were attached per cycle (IV), whereas in processes based on metal chlorides and  $\beta$ -diketonates the growth per cycle is typically  $0.5\text{--}1.5 \text{ at}_{\text{M}} \text{ nm}^{-2}$  (see Table 2.3, p. 21). These differences are explained by the different size and reactivity of the reactants. The van der Waals radius of chlorine is  $0.175 \text{ nm}$ ,<sup>147</sup> corresponding to a maximum theoretical chlorine packing,  $\Delta c_{\text{Cl}}^{\text{max,theor}}$ , of  $9.4 \text{ Cl nm}^{-2}$  (equations 4.15 and 4.16). Assuming  $\theta$  of 0.7 (as determined for the TMA reaction), the maximum expected ligand packing would be  $6.6 \text{ Cl nm}^{-2}$ . Comparison with the values measured for chloride reactants (Table 2.2, p. 20) shows that this ligand packing is not achieved in the reactions of metal chloride reactants (the  $\text{ZrCl}_4$  reaction on alumina being an exception perhaps). The lower packing indicates that here the amount of reactive sites defines saturation, not steric hindrance as in the case of the more reactive TMA. The lower reactivity of metal chlorides with oxide materials is illustrated by the growth of aluminium oxide by ALD from water and  $\text{AlMe}_3$  and from water and  $\text{AlCl}_3$ . At  $300 \text{ }^\circ\text{C}$  the growth is  $0.10 \text{ nm}(\text{cycle})^{-1}$  from  $\text{AlMe}_3$  and only  $0.07 \text{ nm}(\text{cycle})^{-1}$  from  $\text{AlCl}_3$  despite the smaller size of the chloride ligands.<sup>140, 145</sup>

The ligands in metal  $\beta$ -diketonates are larger than the ligands of TMA: thd, acac and methyl ligands have calculated filling areas of  $0.87$ ,<sup>72</sup>  $0.47$ <sup>72</sup> and  $0.14 \text{ nm}^2$ , respectively, corresponding to maximum ligand packing of  $1.1 \text{ thd nm}^{-2}$ ,  $2.1 \text{ acac nm}^{-2}$  and  $7.2 \text{ Me nm}^{-2}$ . The larger ligand size thus partly accounts for the considerably lower

metal loadings achieved with metal  $\beta$ -diketonates than with TMA. Furthermore, metal  $\beta$ -diketonates do not react with all surface OH groups<sup>25,37,84,85</sup> as TMA does, and this increases the difference with TMA further. The lower reactivity of metal  $\beta$ -diketonates with OH groups is illustrated by the growth of aluminium oxide thin films from Al(acac)<sub>3</sub> and ozone. A growth of 0.023 nm(cycle)<sup>-1</sup> is obtained at 350 °C,<sup>148</sup> whereas a growth of 0.044 nm(cycle)<sup>-1</sup> would be expected from equation 4.21 assuming  $\theta$  of 0.7,  $f$  of 1 and  $c_{(O)H}$  of 4 at<sub>H</sub> nm<sup>-2</sup> ( $c_{(O)H}^{eq} \approx 5$  at<sub>H</sub> nm<sup>-2</sup>; ozone can leave the OH group content lower than water does<sup>149</sup>). The observed lower growth per cycle, corresponding to  $f$  of about 0.35, indicates the lower reactivity of Al(acac)<sub>3</sub>.

In the growth of aluminium nitride on silica, new aluminium nitride species were deposited with equal probability on the still-exposed silica and on aluminium nitride species already present on the surface (see Section 4.3.2). Thus, the growth can be visualised as occurring simultaneously laterally and vertically (type (b) in Figure 4.12). Similar simultaneous lateral and vertical growth has been observed in the growth of silica on alumina from HMDS and oxygen.<sup>34</sup> Lateral growth (type (a) in Figure 4.12) has been concluded for the growth of chromia on alumina from Cr(acac)<sub>3</sub> and oxygen,<sup>30</sup> whereas vertical growth (type (c) in Figure 4.12) has been found for the growth of nickel oxide on alumina from Ni(acac)<sub>2</sub> and oxygen.<sup>150</sup> Thus, coverage of the support by the adsorbed species increases in a highly individual way, depending on the support and on the reactants.

# Chapter 5

## Cobalt/AlN/silica catalysts

The preparation of cobalt catalysts on silica and AlN/silica supports by the saturating reaction of  $\text{Co}(\text{acac})_3$  (V,VI) is presented in Section 5.1. The catalytic properties of the Co/silica and Co/AlN/silica materials in the hydroformylation of ethene (VI) are discussed in Section 5.2.

### 5.1 Reaction of $\text{Co}(\text{acac})_3$ with silica and AlN/silica supports

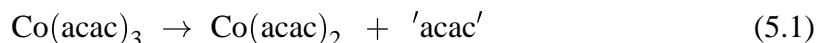
$\text{Co}(\text{acac})_3$  was reacted with silica heat-treated at different temperatures and with silica surfaced in varying degree with aluminium nitride with the purpose of clarifying the mechanisms of  $\text{Co}(\text{acac})_3$  reaction with the various reactive sites: that is, OH groups,  $\text{NH}_x$  groups, oxygen bridges and nitrogen bridges (V,VI). On the basis of previous investigations of the reaction of  $\text{Co}(\text{acac})_3$  with silica<sup>35,59,60</sup> and alumina,<sup>151</sup> 180 °C was chosen as the reaction temperature.

#### 5.1.1 Verification of surface saturation

To investigate whether the reaction of  $\text{Co}(\text{acac})_3$  with silica at 200 °C is saturating, the cobalt loadings in the top and bottom parts of the silica bed were measured as a function of the  $\text{Co}(\text{acac})_3$  dose (V). The cobalt concentration settled to a constant value when the  $\text{Co}(\text{acac})_3$  dose reached  $1.8 \text{ mmol g}_{\text{silica}}^{-1}$  (Figure 2, V), indicating that the reaction is saturating in nature.

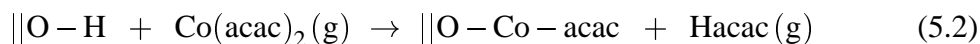
## 5.1.2 Reaction mechanisms

Although cobalt catalysts prepared by the saturating reaction of  $\text{Co}(\text{acac})_3$  have been successfully applied in various reactions,<sup>35,54,59,60,62</sup> the reaction mechanisms involved in the preparation of the catalysts have not been discussed in detail. It appears that  $\text{Co}(\text{acac})_3$  itself did not react with the supports but first transformed to  $\text{Co}(\text{acac})_2$  (V). Several observations indirectly support this interpretation (V): (i) the DRIFT spectra measured for  $\text{Co}(\text{acac})_3$ - and  $\text{Co}(\text{acac})_2$ -modified silica were identical, showing the presence of acac ligands bonded to  $\text{Co}^{2+}$  rather than  $\text{Co}^{3+}$ ; (ii) the amount of cobalt bonded on silica from  $\text{Co}(\text{acac})_3$  and  $\text{Co}(\text{acac})_2$  was the same; (iii) the carbon balance suggests that carbon was lost from the  $\text{Co}(\text{acac})_3$  molecule through another mechanism than ligand exchange; (iv) the TG-DTA measurements carried out for  $\text{Co}(\text{acac})_3$  indicated that, at about 220 °C, a compound with thermal properties resembling those of  $\text{Co}(\text{acac})_2$  began to desorb and (v) the excess reactant collected in cold tubes located after the ALD reactor assumed the violet colour of  $\text{Co}(\text{acac})_2$ .  $\text{Co}(\text{acac})_3$  thus seems to have been transformed to  $\text{Co}(\text{acac})_2$ , according to reaction 5.1 (V).



How this transformation took place is not known in detail.

As indicated by the decrease in the intensity of the OH group bands of silica in the DRIFT results (Figure 4, V), the cobalt reactant, presumably  $\text{Co}(\text{acac})_2$  formed from  $\text{Co}(\text{acac})_3$ , reacted with part of the OH groups. Further indication that the OH groups were involved in the reaction was the decrease in the amount of cobalt bonded to the surface and the increase in acac/Co ratio with increasing heat-treatment temperature (i.e., with decreasing OH group content of silica) as shown in Figure 5.1. For 200 °C silica, the acac/Co ratio after the reaction was about one. On this support, the major reaction mechanism responsible for bonding cobalt species on the surface was most likely the ligand exchange reaction of the  $\text{Co}(\text{acac})_2$ , formed from  $\text{Co}(\text{acac})_3$ , with OH groups of silica (5.2).



For silica heat-treated at 600–750 °C, the acac/Co ratio was well above one (Figure 5.1A), indicating that, on average, less than one acac ligand had been released from the surface per bonded  $\text{Co}(\text{acac})_2$ . Moreover, a comparison of the total OH group content on silica heat-treated at 750 °C, 1.1 OHnm<sup>-2</sup>, with the amount of bonded cobalt, 2.0 at<sub>Co</sub> nm<sup>-2</sup>, shows that reaction with OH groups cannot fully account for the bonding of cobalt species (V). Knowing that in  $\text{Co}(\text{acac})_2$  the central cobalt atom is coordinatively unsaturated, it seems likely that  $\text{Co}(\text{acac})_2$  can bond to silica through association to

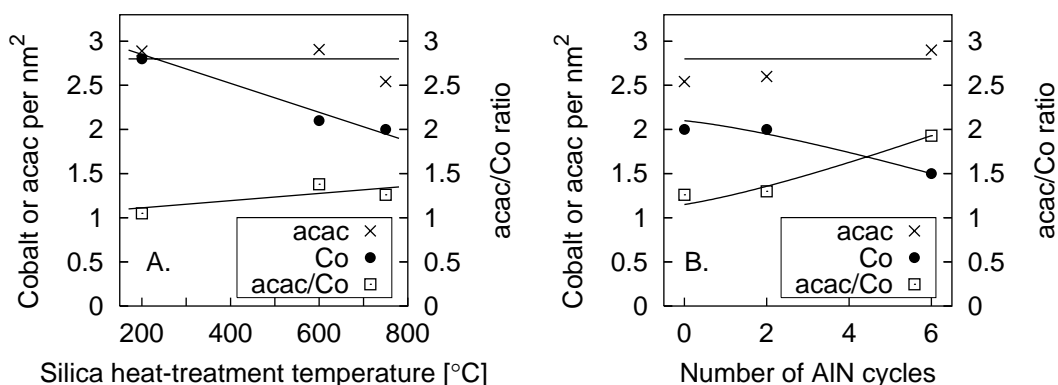
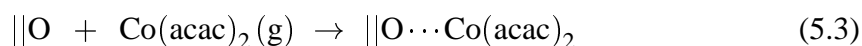


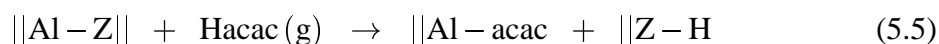
**Figure 5.1:** The average amounts of acac ligands and cobalt bonded in the reaction of  $\text{Co}(\text{acac})_3$  and the acac/Co ratios (A) as a function of heat-treatment temperature of silica and (B) as a function of the extent of aluminium nitride modification of silica (VI).

surface oxygen species (V) (5.3).



The proposed reaction (5.3) is similar to that assigned to  $\text{Cu}(\text{acac})_2$  on silica by Kenvin et al.<sup>152</sup>

On the AlN/silica supports as evidenced by DRIFT spectroscopy, the reaction of the cobalt reactant resulted in the formation of aluminium-bonded acac groups (VI). The formation of aluminium-bonded acac groups can be explained by the occurrence of two types of reactions: dissociative reaction of  $\text{Co}(\text{acac})_2$  (5.4) and dissociative reaction of the Hacac released in the ligand exchange reaction (5.5).



Z denotes either oxygen or nitrogen. The occurrence of reactions 5.4 and 5.5 is supported by the high acac/Co ratio obtained on the 6·AlN/silica support.

### 5.1.3 Factor determining the surface saturation

The amount of acac ligands on the  $\text{Co}(\text{acac})_3$ -modified silica and AlN/silica samples settled at a constant level at saturation,  $2.7 \pm 0.2 \text{ acac nm}^{-2}$  (V, VI). This was true irrespective of the types of bonding sites present on the surface: OH groups,  $\text{NH}_x$  groups, oxygen bridges or nitrogen bridges. Thus the steric hindrance imposed by the acac ligands seems to be the factor determining the saturation of the surface with the adsorbed species.

Figure 5.2 shows a schematic representation of the silica surface after the reaction with  $\text{Co}(\text{acac})_3$ .

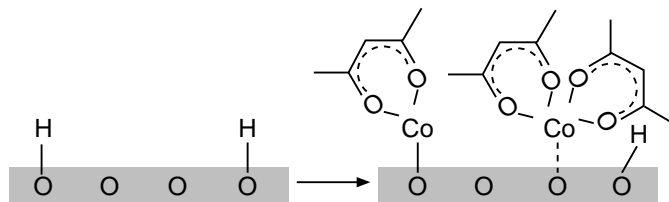


**Figure 5.2:** Schematic representation of the surface reaction products generated in the saturating reaction of  $\text{Co}(\text{acac})_3$  (or, more likely,  $\text{Co}(\text{acac})_2$  formed from  $\text{Co}(\text{acac})_3$ ) with silica (V).

#### 5.1.4 Comparison with other saturating gas–solid reactions

The amount of cobalt bonded in the  $\text{Co}(\text{acac})_3$  reaction followed a decreasing trend with decreasing OH group content of the support similar to the trend observed in almost all saturating gas–solid reactions reported in Table 2.2 (p. 20). However, no quantitative dependence was seen between the amount of cobalt bonded and the OH groups present. Moreover, for surfaces with a low number of OH groups (600 and 750 °C silica), the amount of cobalt bonded exceeded the amount of OH groups. This type of behaviour has not been reported for other metal  $\beta$ -diketonate reactants.

The factor defining the saturation of the reaction of  $\text{Co}(\text{acac})_3$  with silica was concluded to be the steric hindrance imposed by the acac ligands. The acac ligand packing at achieved at saturation was  $2.7 \pm 0.2 \text{ acac nm}^{-2}$  (V, VI), which is the same as obtained by Haukka et al.<sup>151</sup> for the  $\text{Co}(\text{acac})_3$  reaction with alumina ( $2.6 \text{ acac nm}^{-2}$ ). The steric hindrance defining the saturation is the same factor as was observed for the reaction of TMA with oxide supports (Section 4.1.3, p. 32). Most likely, steric hindrance imposed by the ligands also defines the saturation of the reaction of several  $\text{M}(\text{thd})_n$  compounds with alumina ( $\text{M} = \text{Ce}^{4+}, \text{Mn}^{3+}, \text{La}^{3+}, \text{Cu}^{2+}, \text{Mg}^{2+}$ ), since a constant thd ligand packing,  $1.2 \pm 0.1 \text{ thd nm}^{-2}$ , has been observed even though the amount of bound metal varies ( $0.5\text{--}0.8 \text{ at}_M \text{ nm}^{-2}$ ).<sup>33</sup> Such uniform acac ligand packing as for  $\text{M}(\text{thd})_n$  compounds has not been observed for metal acetylacetonates, however. For example, the reaction of  $\text{Cr}(\text{acac})_3$  on alumina gives only  $1.8 \text{ acac nm}^{-2}$ .<sup>30</sup> The question remains, whether the higher acac (i.e., carbon) content obtained from  $\text{Co}(\text{acac})_3$  could have been caused by the decomposition of  $\text{Co}(\text{acac})_3$  further than to  $\text{Co}(\text{acac})_2$ . Such decomposition could result, for example, in acetate ligands,<sup>37</sup> which are smaller than the acac ligands and might thus enable a higher carbon content.

Despite the complexity of the reaction of  $\text{Co}(\text{acac})_3$ , the reaction is characterised by a well-defined saturation level and can be applied in the preparation of cobalt catalysts.<sup>35, 54, 59, 60, 62</sup>

## 5.2 Hydroformylation activity

Before  $\text{Co}(\text{acac})_3$ -modified silica and  $\text{AlN}/\text{silica}$  materials can be used as hydroformylation catalysts, the acac ligands have to be removed and the cobalt has to be reduced. Typically, this is achieved by treatment with hydrogen.<sup>35, 54, 59, 60</sup> According to Backman et al.,<sup>35</sup> a maximum in the hydrogen chemisorption capacity is observed for  $\text{Co}(\text{acac})_3$ -modified silica after hydrogen treatment at 550 °C. This hydrogen treatment temperature was adopted in this work for the  $\text{Co}(\text{acac})_3$ -modified silica and  $\text{AlN}/\text{silica}$  samples (VI).

According to carbon determination, 75% of the carbon present on  $\text{Co}(\text{acac})_3$ -modified 2· $\text{AlN}/\text{silica}$  was removed in the hydrogen treatment at 550 °C (VI). Carbon determinations were not made on other samples. However, temperature-programmed reduction experiments carried out by Backman et al.<sup>35</sup> for  $\text{Co}(\text{acac})_3$ -modified silica showed a hydrogen consumption maximum at about 600 °C, which is attributable to the hydrogenation of carbonaceous species. Together these findings suggest that some residual carbon was present in our  $\text{Co}/\text{silica}$  sample, and most likely also in the  $\text{Co}/6\cdot\text{AlN}/\text{silica}$  sample.

The hydroformylation activity of the  $\text{Co}/n\cdot\text{AlN}/\text{silica}$  catalysts decreased with increasing extent of aluminium nitride modification (Figure 3, VI). The decrease is probably partly explained by the formation of large cobalt particles during the hydrogen treatment at 550 °C. According to hydrogen chemisorption experiments performed at 30 °C, the surface area of metallic cobalt decreases with increasing aluminium nitride modification, which indicates low dispersion of cobalt (VI). The lower dispersion on  $\text{AlN}/\text{silica}$  supports than on silica support was probably due to differences in the mechanism of bonding of the cobalt reactant on the supports. On silica, the acac/Co ratio after the reaction of the cobalt reactant was well below two (see Figure 5.1). The acac/Co ratio increased with the extent of aluminium nitride modification, being two for the 6· $\text{AlN}/\text{silica}$  support. The acac/Co ratio of two enabled the desorption of  $\text{Co}(\text{acac})_2$  from the surface during heating and allowed the formation of larger cobalt particles (VI).

# Chapter 6

## Chromium(III)/AlN/alumina catalysts

Chromium(III)/AlN/alumina samples were prepared by supporting chromium on AlN/alumina by the saturating reaction of  $\text{Cr}(\text{acac})_3$  (VII). For reference, corresponding samples were prepared on alumina. The catalytic properties of the Cr(III)/alumina and Cr(III)/AlN/alumina materials were investigated in the dehydrogenation of isobutane (VII). The preparation of catalysts from  $\text{Cr}(\text{acac})_3$  is discussed in Section 6.1, and the catalytic properties of the Cr(III)/alumina and Cr(III)/AlN/alumina materials are discussed in Section 6.2.

### 6.1 Reaction of $\text{Cr}(\text{acac})_3$ with alumina and AlN/alumina supports

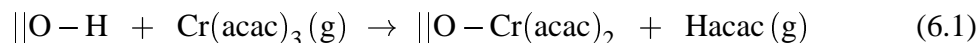
$\text{Cr}(\text{acac})_3$  was reacted with alumina heat-treated at 200–800 °C and with alumina supports surfaced in different degree with aluminium nitride with the purpose of clarifying the mechanisms of reaction of  $\text{Cr}(\text{acac})_3$  with the various reactive sites (VII). A reaction temperature of 200 °C was chosen on the basis of previous investigations.<sup>30,37,93</sup>

#### 6.1.1 Verification of surface saturation

A  $\text{Cr}(\text{acac})_3$  dose of about  $1.2 \text{ mmol g}_{\text{alumina}}^{-1}$  was used in the work (VII). According to Kytökivi et al.,<sup>30,93</sup> this amount is sufficient for saturating the alumina surface with the adsorbed species. That surface saturation had been achieved was confirmed by measurement of the same chromium contents in the top and bottom parts of the support bed and by the uniform colour of the samples (VII).

## 6.1.2 Reaction mechanisms

Kytökivi and Hakuli and their coauthors<sup>30,37</sup> concluded that ligand exchange reaction of  $\text{Cr}(\text{acac})_3$  with OH groups (6.1) was the main reaction mechanism in the chemisorption of  $\text{Cr}(\text{acac})_3$  on alumina at 200 °C.



The findings of the present work are in agreement with the earlier findings in regard to the occurrence of the ligand exchange reaction (6.1). As shown in Figure 6.1, an acac/Cr ratio below three is observed for 200 °C alumina, and DRIFT spectroscopy indicates interaction between OH groups and  $\text{Cr}(\text{acac})_3$  (VII). However, the acac/Cr ratios measured for other samples were about three (Figure 6.1), as opposed to the value of two reported by Kytökivi and Hakuli and their coauthors.<sup>30,37</sup> One or more other reaction mechanisms, which can account for the bonding of all the acac ligands of chromium on the surface, must thus be taken into account.

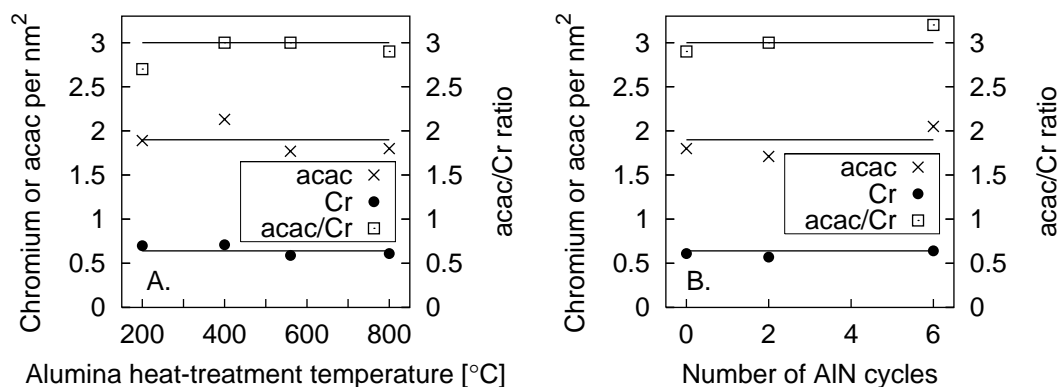
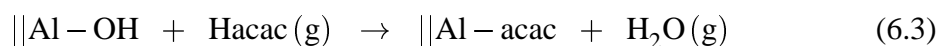
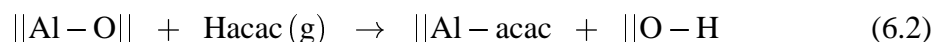


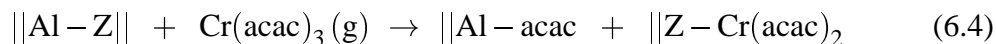
**Figure 6.1:** Average amounts of acac ligands and chromium bonded in the chemisorption of  $\text{Cr}(\text{acac})_3$  and the acac/Cr ratios (A) as a function of heat-treatment temperature on alumina and (B) as a function of the extent of aluminium nitride modification on AlN/alumina (VII).

One additional reaction mechanism that could result in acac/Cr ratios of three is a secondary reaction of the Hacac released in reaction 6.1 with c.u.s. Al–O pairs (6.2) or with OH groups (6.3) on the surface.

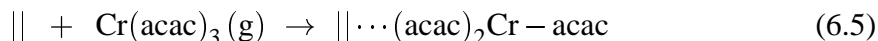


With both these reaction mechanisms (6.2, 6.3) being operative, Hacac chemisorbs on alumina in a saturating manner, resulting in an acac group content of  $2.1 \pm 0.1 \text{ acac nm}^{-2}$ .<sup>153</sup>

Another possibility is the dissociation of  $\text{Cr}(\text{acac})_3$  in oxygen or nitrogen bridges on the surface (6.4).



Yet a third possibility would be an associative adsorption of  $\text{Cr}(\text{acac})_3$  (6.5), which Babich et al.<sup>88</sup> concluded to be the main chemisorption mechanism of  $\text{Cr}(\text{acac})_3$  on alumina at 190 °C.



The secondary reaction of Hacac and the dissociative adsorption of  $\text{Cr}(\text{acac})_3$  both would result in acac ligands bonded to aluminium as well as chromium, whereas associative adsorption would result bonding of acac ligands only to chromium. Because, according to DRIFT results (Figure 2, VII), both chromium- and aluminium-bonded acac ligands were present, secondary reactions of Hacac (6.2, 6.3) or dissociation of  $\text{Cr}(\text{acac})_3$  (6.4) or both mechanisms must have been operative, certainly not association (6.5) alone (VII).

On the basis of ESR measurements, bonding of chromium to the surface exclusively through reactions 6.1, 6.4 and 6.5 would seem to be a simplification (VII). Reactions 6.1, 6.4 and 6.5 would result in chromium atoms that are atomically dispersed on the surface. The ESR spectra indicate that, in addition to atomically dispersed  $\text{Cr}^{3+}$  species, some cluster-type  $\text{Cr}^{3+}$  was present (Figure 3, VII). Some decomposition of the acac ligands may thus have taken place, as noted by Hakuli et al.<sup>85</sup> for the  $\text{Cr}(\text{acac})_3$  reaction with silica at 220 °C and above.

### 6.1.3 Factor determining the surface saturation

In the chemisorption of  $\text{Cr}(\text{acac})_3$ , the acac ligand content was at the same level,  $1.9 \pm 0.2 \text{ acac nm}^{-2}$ , regardless of the nature and number of reactive sites on the support (VII). At the same time the chromium content was constant at  $0.64 \pm 0.06 \text{ at}_{\text{Cr}} \text{ nm}^{-2}$  (VII). The acac ligand content was the same as obtained in the chemisorption of Hacac at 200 °C on alumina,  $2.1 \pm 0.2 \text{ acac nm}^{-2}$ .<sup>153</sup> Evidently, then, it is the steric hindrance imposed by the acac ligands that defines the saturation of the surface with the adsorbed species. The reaction of  $\text{Cr}(\text{acac})_3$  with alumina and AlN/alumina is schematically illustrated in Figure 6.2.

### 6.1.4 Comparison with other saturating gas–solid reactions

The reaction of  $\text{Cr}(\text{acac})_3$  with alumina is an exception among the reactions of metal  $\beta$ -diketonates, since the amount of chromium attached remains constant with decreasing OH

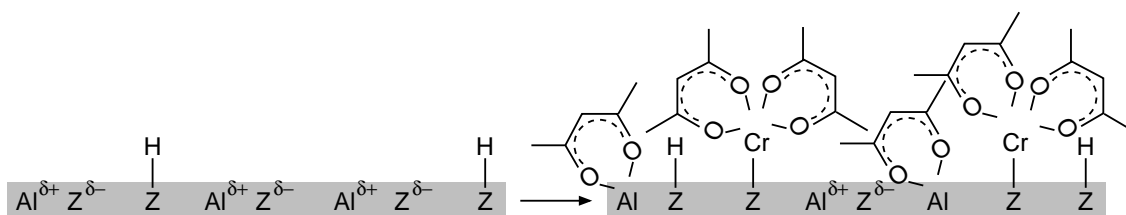


**Figure 6.2:** Schematic representation of the surface reaction products generated in the saturating reaction of  $\text{Cr}(\text{acac})_3$  with alumina and AlN/alumina (VII).

group content of the support ( $0.64 \pm 0.06 \text{ at}_{\text{Cr}} \text{ nm}^{-2}$ ) (VII).<sup>88,93</sup> Typically, the amount of metal attached decreases with decreasing OH group content of the support (see Table 2.2, p. 20).

The same factor was concluded to determine the saturation of the surface with adsorbed species for the  $\text{Cr}(\text{acac})_3$  reaction as for the TMA reaction (Section 4.1.3, p. 32) and for  $\text{Co}(\text{acac})_2$ , formed from  $\text{Co}(\text{acac})_3$  (Section 5.1.3, p. 51). That factor is the steric hindrance imposed by the ligands. It remains somewhat unclear whether there is a general level at which the acac ligand content will settle when steric hindrance defines saturation. The finding of approximately the same acac ligand content in the saturating reaction of Hacac with alumina,  $2.1 \pm 0.1 \text{ acac nm}^{-2}$ ,<sup>153</sup> the  $\text{Ni}(\text{acac})_2$  reaction on silica and alumina,  $2.2 \text{ acac nm}^{-2}$ ,<sup>154</sup> and the  $\text{Cr}(\text{acac})_3$  reaction with alumina,  $1.9 \pm 0.2 \text{ acac nm}^{-2}$ , would suggest that about two acac per square nanometre is generally valid. The reaction of  $\text{Co}(\text{acac})_3$  on silica and alumina nevertheless gives a higher acac ligand content, as can the reaction of  $\text{Ni}(\text{acac})_2$  on alumina,<sup>29</sup> questioning the foundations of this conclusion.

## 6.2 Dehydrogenation activity

The activity of chromium catalysts prepared on alumina and AlN/alumina supports was investigated in isobutane dehydrogenation (VII). In comparison with the loadings reported in Figure 2.4 (p. 23), the chromium loadings of the catalysts prepared from  $\text{Cr}(\text{acac})_3$  were rather low, and the chromium species were probably mostly isolated, in direct contact with the support.

Before the testing, the acac ligands remaining in the  $\text{Cr}(\text{acac})_3$ -modified samples were removed by an ammonia treatment at  $550 \text{ }^\circ\text{C}$ . The ammonia treatment was slightly less efficient in removing the acac ligands than was oxygen or water treatment at the same temperature: it left behind residual carbon, in an amount that increased with the extent of aluminium nitride modification of the support (VII).

The use of an AlN/alumina support instead of an alumina support did not affect the

amount of cracking products ( $C_1$ – $C_3$  hydrocarbons), in contrast to what was anticipated (VII). However, about the same amount of cracking products was obtained with and without catalyst (Figure 6, VII), indicating that the cracking products were generated in thermal reactions.

Compared with other supports (alumina and 2·AlN/alumina), the use of a 6·AlN/alumina support decreased the dehydrogenation activity of the fresh chromium catalysts (Figure 6.3). The decrease was more than could be explained by the carbon remaining after ligand removal (VII). The lower activity would seem to indicate that the replacement of Cr–O pairs with Cr–N pairs has a negative effect on activity (VII): the probability of finding an oxygen ion nearby a chromium ion is much lower for the catalyst prepared on the 6·AlN/alumina support than for other catalysts since, according to LEIS, aluminium nitride covers about 74% of the support (IV). The conclusion that Cr–O pairs are more active than Cr–N pairs is supported by the marked increase in the activity of the Cr/6·AlN/alumina catalyst after the oxidative regeneration, which at least partly destroyed the nitride structure of the support (VII).

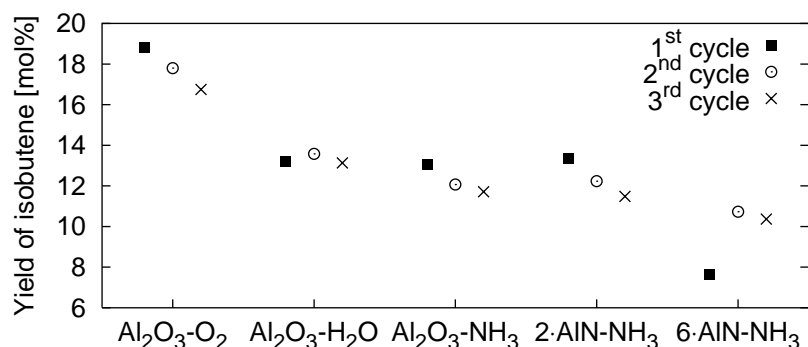


**Figure 6.3:** Activity of chromium catalysts prepared from  $Cr(acac)_3$  on the indicated supports, with ligands removed by  $O_2$ ,  $H_2O$  or  $NH_3$ , as indicated (VII).

For catalysts prepared on alumina, the catalyst where ligands were removed by oxygen was considerably more active than catalysts where ligands were removed by water or ammonia (Figure 6.3). The water and ammonia treatments seem to have produced chromium sites that were less active in dehydrogenation than the sites produced by oxygen treatment (VII). The reason for this is not clear but the following can be suggested. The oxygen treatment oxidised part of the chromium to  $Cr^{6+}$  (VII), which is more mobile than  $Cr^{3+}$ —for example, it dissolves in aqueous/basic medium.<sup>37, 111–113</sup> During oxygen treatment the  $Cr^{6+}$  ions may have formed clusters, which have been suggested to possess higher dehydrogenation activity than isolated chromium sites.<sup>56, 113, 119</sup> ESR confirmed the formation of small chromia clusters during the oxygen treatment (VII).

# Chapter 7

## Conclusions

The surfaces of porous oxide materials can be modified with nitrides in a controlled manner by the ALD technique, that is, by repeated separate, saturating gas–solid reactions. This work has demonstrated the preparation of aluminium nitride from TMA and ammonia on porous silica and alumina. In one reaction cycle of TMA at 150 °C and ammonia at 550 °C, an average growth of 2.4 AlN units was obtained per square nanometer of the support, six reaction cycles resulting in a coverage of 74% of the support with aluminium nitride. TMA was found to react with all surface hydrogen atoms present in OH or NH<sub>x</sub> groups, releasing methane, and additionally with surface oxygen and nitrogen bridges. Steric hindrance imposed by the ligands defined the saturation of the surface with adsorbed species; at saturation, the methyl group packing was 5–6 Me nm<sup>-2</sup>. Ammonia replaced the methyl groups present on TMA-modified surfaces with NH<sub>x</sub> groups ( $x = 2, 1$  or  $0$ ). The growth per cycle of aluminium nitride was higher than reported for the ALD processing of other materials on porous supports, evidently because of the high reactivity of TMA and small size of the methyl ligands.

The results of the TMA reaction agreed quantitatively with the results obtained by others in ALD thin film growth of aluminium oxide. This agreement encouraged the derivation of a model relating the size and reactivity of a metal reactant to growth per cycle of the corresponding oxide material by ALD.

Cobalt and chromium catalysts were prepared by ALD on AlN/silica and AlN/alumina supports, respectively, and on the corresponding oxides. In the preparation of the catalysts from Co(acac)<sub>3</sub> and Cr(acac)<sub>3</sub>, the factor defining the saturation of the reaction was the same as on the oxide supports: steric hindrance imposed by the ligands. The amount of cobalt attached from Co(acac)<sub>3</sub> depended on the amount of OH groups on the surface (1.5–2.8 at<sub>Co</sub> nm<sup>-2</sup>), whereas the amount of chromium attached from Cr(acac)<sub>3</sub> did not depend on it (ca. 0.6 at<sub>Cr</sub> nm<sup>-2</sup>). Dissociative and associative reactions of the metal ace-

tylacetate reactants and of the Hacac released in ligand exchange reaction took place on the AlN/oxide supports. This was found to be a disadvantage for the Co/AlN/silica catalysts, as the high acac/Co ratio of the surface complex enabled the desorption of  $\text{Co}(\text{acac})_2$  during catalytic testing, resulting in large cobalt particles and low hydroformylation selectivity.

The activity of Cr(III)/AlN/alumina catalysts prepared in one reaction cycle of  $\text{Cr}(\text{acac})_3$  was evaluated in isobutane dehydrogenation at 580 °C. The amount of cracking products was not affected by the type of support, as the products were mainly formed in thermal reactions. The use of AlN/alumina supports in place of alumina supports decreased the dehydrogenation activity of chromium catalysts. This indicates that, for active chromium catalysts, Cr–O pairs are required and the use of nitrogen does not enhance the activity.

Although the use of aluminium nitride surfaced supports did not offer additional benefits for catalytic activity in the reactions tested in this work, for reactions carried out in the absence of oxygen-containing compounds, and perhaps at moderate temperatures, the aluminium nitride surfaced supports might prove useful. Moreover, the information obtained will be useful in the future investigations of the growth of aluminium nitride and of other materials by ALD and in the identification of the active sites on dehydrogenation catalysts.

# List of abbreviations and symbols

$a$	Lattice constant of anions A of material $BA_x$ in a square surface lattice in the model of Ylilammi, <sup>145</sup> nm
Acac	Acetylacetonate (pentane-2,4-dionate), $C_5H_7O_2^-$
$a_L$	Filling area of ligand L, $nm^2$
ALCVD <sup>TM</sup>	Atomic layer chemical vapour deposition
ALD	Atomic layer deposition
ALE	Atomic layer epitaxy
AlN	Aluminium nitride
at	Atom
$c_i$	Surface loading of atom $i$ , $at_i nm^{-2}$ (atoms $i$ per square nanometer)
$c_i^{wt\%}$	Concentration of compound $i$ , wt%
$c_{(O)H}$	Content of hydrogen in OH groups on a material, $at_H nm^{-2}$
$c_{(O)H}^{eq}$	Content of hydrogen in OH groups on a material at equilibrium at a certain temperature, $at_H nm^{-2}$
CPMAS	Cross-polarisation magic angle spinning
c.u.s.	Coordinatively unsaturated
CVD	Chemical vapour deposition
DTA	Differential thermal analysis
DRIFT	Diffuse reflectance Fourier transform infrared (spectroscopy)

EDS	Energy-dispersive X-ray spectroscopy
ESR	Electron spin resonance (spectroscopy)
$f$	Fraction of hydrogen atoms in OH groups that react with $ML_n$ reactant
Hacac	Acetylacetone (pentane-2,4-dione), $C_5H_8O_2$
HMDS	Hexamethyl disilazane, $((CH_3)_3Si)_2NH$
L	Ligand in the $ML_n$ reactant
LEIS	Low energy ion scattering
M	Metal atom
$M_i$	Molar mass of component $i$ , $g\ mol^{-1}$
MAS	Magic angle spinning
Me	Methyl group, $-CH_3$
$ML_n$	Model reactant consisting of a metal atom, $M^{n+}$ , and $n$ ligands, $L^-$
$n$	Number of ligands in the $ML_n$ reactant
$N_A$	Avogadro's number, $6.022 \times 10^{23}$ (atoms) $mol^{-1}$
NMR	Nuclear magnetic resonance (spectroscopy)
$p$	Packing efficiency in ALD growth in the model of Ylilammi <sup>145</sup>
$r_L$	Radius of ligand L, nm
$S$	Specific surface area, $m^2\ g^{-1}$
SEM	Scanning electron microscopy
TG	Thermogravimetry
Thd	2,2,6,6-Tetramethyl-3,5-heptanedionate, $C_{11}H_{19}O_2^-$
$Ti(OPr^i)_4$	Titanium isopropoxide, $Ti(OCH(CH_3)_2)_4$
TMA	Trimethylaluminium, $AlMe_3$ , $Al(CH_3)_3$
WHSV	Weight hourly space velocity, $h^{-1}$

XRD	X-ray diffraction
XRF	X-ray fluorescence (spectroscopy)
Z	Oxygen or nitrogen atom
$\Delta c_L$	Increase in the surface loading of ligands L in a saturating reaction of $ML_n$ , $L\text{ nm}^{-2}$
$\Delta c_L^{\text{maxtheor}}$	Theoretical maximum for the ligand packing at saturation, $L\text{ nm}^{-2}$
$\Delta c_M$	Increase in the surface loading of metal M in a saturating reaction of $ML_n$ , $\text{at}_M\text{ nm}^{-2}$
$\Delta c_{(\text{O})\text{H}}$	Amount of hydrogen atoms in OH groups, consumed in the reaction of $ML_n$ , $\text{at}_H\text{ nm}^{-2}$
$\Delta h_{\text{MO}_x}$	Increase in film thickness of $\text{MO}_x$ material in one ALD reaction cycle, $\text{nm}(\text{cycle})^{-1}$
$v_{\text{MO}_x}$	Atomic density of material $\text{MO}_x$ , $\text{nm}^{-3}$
$\rho_{\text{MO}_x}$	Density of material $\text{MO}_x$ , $\text{g nm}^{-3}$ (i.e., $10^{-21} \times \rho [\text{g cm}^{-3}]$ )
$\theta$	Coverage of ligands L at saturation; $\Delta c_L / \Delta c_L^{\text{maxtheor}}$
	Surface site

## References

- [1] Weckhuysen, B. M., Wachs, I. E. and Schoonheydt, R. A., Surface chemistry and spectroscopy of chromium in inorganic oxides, *Chem. Rev.* **96** (1996) 3327–3349.
- [2] Knözinger, H. and Ratnasamy, P., Catalytic aluminas: surface models and characterization of surface sites, *Catal. Rev.—Sci. Eng.* **17** (1978) 31–69.
- [3] Cao, S.-K., Huang, M.-Y. and Jiang, Y.-Y., Hydroformylation of heptene-1 catalyzed by some inorganic polymer–metal complexes, *J. Macromol. Sci., Chem. A* **26** (1989) 381–389.
- [4] Benitez, J. J., Odriozola, J. A., Marchand, R., Laurent, Y. and Grange, P., Surface basicity of a new family of catalysts: aluminophosphate oxynitride (AlPON), *J. Chem. Soc., Faraday Trans.* **91** (1995) 4477–4479.
- [5] Méthivier, C., Massardier, J. and Bertolini, J. C., Pd/Si<sub>3</sub>N<sub>4</sub> catalysts: preparation, characterization and catalytic activity for the methane oxidation, *Appl. Catal., A* **182** (1999) 337–344.
- [6] Centeno, M. A., Debois, M. and Grange, P., Platinum aluminophosphate oxynitride (Pt–AlPON) catalysts for the dehydrogenation of isobutane to isobutene, *J. Catal.* **192** (2000) 296–306.
- [7] Delsarte, S., Maugé, F. and Grange, P., Isobutane dehydrogenation over supported platinum acid–base AlGaPON catalysts, *J. Catal.* **202** (2001) 1–13.
- [8] Hullmann, D., Wendt, G., Šingliar, U. and Ziegenbald, G., Propane dehydrogenation over supported platinum silicon nitride catalysts, *Appl. Catal., A* **225** (2002) 261–270.
- [9] Keller, N., Pham-Huu, C., Roy, S., Ledoux, M. J., Estournes, C. and Guille, J., Influence of the preparation conditions on the synthesis of high surface area SiC for use as a heterogeneous catalyst support, *J. Mater. Sci.* **34** (1999) 3189–3202.

- [10] Parmentier, J., Patarin, J., Dentzer, J. and Vix-Guterl, C., Formation of SiC via carbothermal reduction of a carbon-containing mesoporous MCM-48 silica phase: a new route to produce high surface area SiC, *Ceram. Int.* **28** (2002) 1–7.
- [11] Jong, K. P. D. and Geus, J. W., Carbon nanofibers: catalytic synthesis and applications, *Catal. Rev.—Sci. Eng.* **42** (2000) 481–510.
- [12] Salmi, T., Mäki-Arvela, P. M., Toukoniitty, E., Neyestanaki, A. K., Tiainen, L. P., Lindfors, L. E., Sjöholm, R. and Laine, E., Liquid-phase hydrogenation of citral over an immobile silica fibre catalyst, *Appl. Catal., A* **196** (2000) 93–102.
- [13] Karinen, R. S., Krause, A. O. I., Ekman, K., Sundell, M. and Peltonen, R., Etherification over a novel acid catalyst, *Proc. 12th ICC, Granada, Spain, July 2000*, Eds. A. Corma, F. V. Melo, S. Mendioroz and J. L. G. Fierro, Vol. 130 of *Stud. Surf. Sci. Catal.*, Elsevier, Amsterdam 2000, pp. 3411–3416.
- [14] Safronov, V. M., Fasman, A. B. and Vorob'eva, V. I., Hydrogenation of organic compounds on platinum and palladium supported on aluminum nitride. I. Hydrogenation of acetylene derivatives., *Izv. Akad. Nauk Kaz. SSR, Ser. Khim.* **6** (1982) 37–42. In Russian.
- [15] Fripiat, N. and Grange, P., A preliminary study of the *n*-heptane conversion over supported platinum acid–base ZrPON catalysts, *Catal. Lett.* **62** (1999) 53–57.
- [16] Yuan, Y. X., Huang, M. Y. and Jiang, Y. Y., Isomerization of olefins catalyzed by silica-polyalumazine-palladium complexes, *J. Macromol. Sci., Chem. A* **24** (1987) 261–268.
- [17] Kiviaho, J., Hanaoka, T., Kubota, Y. and Sugi, Y., Heterogeneous palladium catalysts for the Heck reaction, *J. Mol. Catal., A* **101** (1995) 25–31.
- [18] Weimer, A. W., Cochran, G. A., Eisman, G. A., Henley, J. P., Hook, B. D., Mills, L. K., Guiton, T. A., Knudsen, A. K., Nicholas, N. R., Volmering, J. E. and Moore, W. G., Rapid process for manufacturing aluminum nitride powder, *J. Am. Ceram. Soc.* **77** (1994) 3–18.
- [19] Sauls, F. C., Hurley, Jr., W. J., Interrante, L. V., Marchetti, P. S. and Maciel, G. E., Effects of ammonia on the pyrolytic decomposition of alkylaluminum amides to aluminum nitride, *Chem. Mater.* **7** (1995) 1361–1368.
- [20] Volpe, L. and Boudart, M., Topotactic preparation of powders with high specific surface area, *Catal. Rev.—Sci. Eng.* **27** (1985) 515–538.

- [21] Fripiat, N., Conanec, R., Marchand, R., Laurent, Y. and Grange, P., Synthesis and characterization of a new oxynitride catalyst: the ZrPON solids, *J. Eur. Ceram. Soc.* **17** (1997) 2011–2015.
- [22] Delsarte, S., Peltier, V., Laurent, Y. and Grange, P., X-ray photoelectron study of new mixed oxynitrides 'AlGaPON', *J. Eur. Ceram. Soc.* **18** (1998) 1287–1291.
- [23] Suntola, T., Atomic layer epitaxy, In *Handbook of Crystal Growth*, Ed. D. T. J. Hurle, Vol. 3, Elsevier, Amsterdam 1994, pp. 601–663.
- [24] Lakomaa, E.-L., Atomic layer epitaxy (ALE) on porous substrates, *Appl. Surf. Sci.* **75** (1994) 185–196.
- [25] Haukka, S., Lakomaa, E.-L. and Suntola, T., Adsorption controlled preparation of heterogenous catalysts, In *Adsorption and its Applications in Industry and Environmental Protection*, Ed. A. Dabrowski, Vol. 120A of *Stud. Surf. Sci. Catal.*, Elsevier, Amsterdam 1999, pp. 715–750.
- [26] Ritala, M. and Leskelä, M., Atomic layer deposition, In *Handbook of Thin Film Materials*, Ed. H. S. Nalwa, Vol. 1, Academic Press, San Diego 2002, pp. 103–159.
- [27] Ritala, M., Leskelä, M., Dekker, J.-P., Mutsaers, C., Soininen, P. J. and Skarp, J., Perfectly conformal TiN and Al<sub>2</sub>O<sub>3</sub> films deposited by atomic layer deposition, *Chem. Vap. Deposition* **5** (1999) 7–9.
- [28] Lakomaa, E.-L., Haukka, S. and Suntola, T., Atomic layer growth of TiO<sub>2</sub> on silica, *Appl. Surf. Sci.* **60/61** (1992) 742–748.
- [29] Lindblad, M., Lindfors, L. P. and Suntola, T., Preparation of Ni/Al<sub>2</sub>O<sub>3</sub> catalysts from vapor phase by atomic layer epitaxy, *Catal. Lett.* **27** (1994) 323–336.
- [30] Kytökivi, A., Jacobs, J.-P., Hakuli, A., Meriläinen, J. and Brongersma, H. H., Surface characteristics and activity of chromia/alumina catalysts prepared by atomic layer epitaxy, *J. Catal.* **162** (1996) 190–197.
- [31] Kytökivi, A., Lakomaa, E.-L., Root, A., Österholm, H., Jacobs, J.-P. and Brongersma, H. H., Sequential saturating reactions of ZrCl<sub>4</sub> and H<sub>2</sub>O vapors in the modification of silica and  $\gamma$ -alumina with ZrO<sub>2</sub>, *Langmuir* **13** (1997) 2717–2725.

- [32] Lindblad, M., Haukka, S., Kytökivi, A., Lakomaa, E.-L., Rautiainen, A. and Suntola, T., Processing of catalysts by atomic layer epitaxy: modification of supports, *Appl. Surf. Sci.* **121/122** (1997) 286–291.
- [33] Haukka, S. and Suntola, T., Advanced materials processing by adsorption control, *Interface Sci.* **75** (1997) 119–128.
- [34] Lindblad, M. and Root, A., Atomically controlled preparation of silica on alumina, *Preparation of Catalysts VII. Proc. 7th Int. Symp. "Scientific Bases for the Preparation of Heterogeneous Catalysts," Louvain-la-Neuve, Belgium, September 1998*, Eds. B. Delmon, P. A. Jacobs, R. Maggi, J. A. Martens, P. Grange and G. Poncelet, Vol. 118 of *Stud. Surf. Sci. Catal.*, Elsevier, Amsterdam 1998, pp. 817–826.
- [35] Backman, L. B., Rautiainen, A., Krause, A. O. I. and Lindblad, M., A novel Co/SiO<sub>2</sub> catalyst for hydrogenation, *Catal. Today* **43** (1998) 11–19.
- [36] Schrijnemakers, K., Impens, N. R. E. N. and Vansant, E. F., Deposition of a titania coating on silica by means of the chemical surface coating, *Langmuir* **15** (1999) 5807–5813.
- [37] Hakuli, A., Kytökivi, A. and Krause, A. O. I., Dehydrogenation of *i*-butane on CrO<sub>x</sub>/Al<sub>2</sub>O<sub>3</sub> catalysts prepared by ALE and impregnation techniques, *Appl. Catal., A* **190** (2000) 219–232.
- [38] Manasevit, H. M., Erdmann, F. M. and Simpson, W. I., The use of metalorganics in the preparation of semiconductor materials. IV. The nitrides of aluminum and gallium, *J. Electrochem. Soc.* **118** (1971) 1864–1868.
- [39] Eichhorn, G. and Rensch, U., MOCVD of AlN on silicon, *Phys. Stat. Solidi A* **19** (1982) K3–K6.
- [40] Rensch, U. and Eichhorn, G., Investigations of the structure of MOCVD AlN layers on silicon, *Phys. Stat. Solidi A* **77** (1983) 195–199.
- [41] Interrante, L. V., Sigel, G. A., Garbaskas, M., Hejna, C. and Slack, G. A., Organometallic precursors to AlN: synthesis and crystal structures of [(CH<sub>3</sub>)<sub>2</sub>AlNH<sub>2</sub>]<sub>3</sub> and the planar species [(*t*-C<sub>4</sub>H<sub>9</sub>)<sub>2</sub>AlNH<sub>2</sub>]<sub>3</sub>, *Inorg. Chem.* **28** (1989) 252–257.
- [42] Sauls, F. C., Interrante, L. V. and Jiang, Z., Me<sub>3</sub>Al·NH<sub>3</sub> formation and pyrolytic methane loss: thermodynamics, kinetics, and mechanism, *Inorg. Chem.* **29** (1990) 2989–2996.

- [43] Mayer, T. M., Rogers, Jr., J. W. and Michalske, T. A., Mechanism of nucleation and atomic layer growth of AlN on Si, *Chem. Mater.* **3** (1991) 641–646.
- [44] Bartram, M. E., Michalske, T. A., Rogers, Jr., J. W. and Mayer, T. M., Chemisorption of trimethylaluminum and ammonia on silica: mechanisms for the formation of Al–N bonds and the elimination of methyl groups bonded to aluminum, *Chem. Mater.* **3** (1991) 953–960.
- [45] Bartram, M. E., Michalske, T. A., Rogers, Jr., J. W. and Paine, R. T., Nucleation and growth of AlN: self-limiting reactions and the regeneration of active sites using sequential exposures of trimethylaluminum and ammonia on silica at 600 K, *Chem. Mater.* **5** (1993) 1424–1430.
- [46] Bertolet, D. C. and Rogers, Jr., J. W., Mechanistics of early stage growth of AlN on alumina: TMAI and NH<sub>3</sub>, *Chem. Mater.* **5** (1993) 391–395.
- [47] Bertolet, D. C., Liu, H. and Rogers, Jr., J., Mechanistics of early stage growth of AlN on alumina. 2. TMAI and NH<sub>3</sub>, *Chem. Mater.* **5** (1993) 1814–1818.
- [48] Liu, H., Bertolet, D. C. and Rogers, Jr., J. W., The surface chemistry of aluminium nitride MOCVD on alumina using trimethylaluminum and ammonia as precursors, *Surf. Sci.* **320** (1994) 145–160.
- [49] Liu, H., Bertolet, D. C. and Rogers, Jr., J. W., Reactions of trimethylaluminum and ammonia on alumina at 600 K—surface chemical aspects of AlN thin film growth, *Surf. Sci.* **340** (1995) 88–100.
- [50] Chen, C. H., Liu, H., Steigerwald, D., Imler, W., Kuo, C. P., Craford, M. G., Ludowise, M., Lester, S. and Amano, J., A study of parasitic reactions between NH<sub>3</sub> and TMGa or TMAI, *J. Electron. Mater.* **25** (1996) 1004–1008.
- [51] Riihelä, D., Ritala, M., Matero, R., Leskelä, M., Jokinen, J. and Haussalo, P., Low temperature deposition of AlN films by an alternate supply of trimethylaluminum and ammonia, *Chem. Vap. Deposition* **2** (1996) 277–283.
- [52] Soto, C., Boiadjev, V. and Tysoe, W. T., Spectroscopic study of AlN film formation by the sequential reaction of ammonia and trimethylaluminum on alumina, *Chem. Mater.* **8** (1996) 2359–2365.
- [53] Elers, K.-E., Ritala, M., Leskelä, M. and Johansson, L.-S., Atomic layer epitaxy growth of AlN thin films, *J. Phys. IV.* **5** (1995) C5–1021–C5–1027.

- [54] Kainulainen, T. A., Niemelä, M. K. and Krause, A. O. I., Ethene hydroformylation on Co/SiO<sub>2</sub> catalysts, *Catal. Lett.* **53** (1998) 97–101.
- [55] Keränen, J., Auroux, A., Ek-Härkönen, S. and Niinistö, L., Calorimetric measurements of the acidity of supported vanadium oxides prepared by ALE and impregnation, *Thermochim. Acta* **379** (2001) 233–239.
- [56] Airaksinen, S. M. K., Kanervo, J. M. and Krause, A. O. I., Deactivation of CrO<sub>x</sub>/Al<sub>2</sub>O<sub>3</sub> catalysts in the dehydrogenation of *i*-butane, *Natural Gas Conversion VI. Proc. 6th Natural Gas Conversion Symposium, Alaska, USA, June 2001*, Eds. E. Iglesia, J. Spivey and T. Fleisch, Vol. 136 of *Stud. Surf. Sci. Catal.*, Elsevier, Amsterdam 2001, pp. 153–158.
- [57] Keränen, J., Auroux, A., Ek, S. and Niinistö, L., Preparation, characterization and activity testing of vanadia catalysts deposited onto silica and alumina supports by atomic layer deposition, *Appl. Catal., A* **228** (2002) 213–225.
- [58] Smeds, S., Salmi, T., Lindfors, L. P. and Krause, A. O. I., Chemisorption and TPD studies of hydrogen on Ni/Al<sub>2</sub>O<sub>3</sub>, *Appl. Catal., A* **144** (1996) 177–194.
- [59] Backman, L. B., Rautiainen, A., Lindblad, M. and Krause, A. O. I., Effect of support and calcination on the properties of cobalt catalysts prepared by gas phase deposition, *Appl. Catal., A* **191** (2000) 55–68.
- [60] Backman, L. B., Rautiainen, A., Lindblad, M., Jylhä, O. and Krause, A. O. I., Characterisation of Co/SiO<sub>2</sub> catalysts prepared from Co(acac)<sub>3</sub> by gas phase deposition, *Appl. Catal., A* **208** (2001) 223–234.
- [61] Hietala, J., Knuuttila, P. and Kytökivi, A., Catalyst for metathetic reactions of olefins, *Patent EP 0 524 522*, Neste Oy, 27 January 1993.
- [62] Milt, V. G., Ulla, M. A. and Lombardo, E. A., Zirconia-supported cobalt as catalyst for methane combustion, *J. Catal.* **200** (2001) 241–249.
- [63] Baltés, M., Kytökivi, A., Weckhuysen, B. M., Schoonheydt, R. A., Van Der Voort, P. and Vansant, E. F., Supported tantalum oxide and supported vanadia–tantalum mixed oxides: structural characterization and surface properties, *J. Phys. Chem. B* **105** (2001) 6211–6220.
- [64] Hokkanen, H., *Comparison of liquid and gas phase methods for catalyst preparation*, M.Sc. thesis, Helsinki University of Technology, Espoo, 1991, 110 p. In Finnish.

- [65] Knuutila, H. and Lakomaa, E.-L., Polymerization catalyst for olefins, *Patent US 5 290 748*, Neste Oy, 1 March 1994.
- [66] Tiitta, M., Turunen, H., Aittamaa, J., Ilme, J., Isokoski, K., Kytökivi, A., Kylmämetsä, H., Lakomaa, E.-L., Lindblad, M. and Hölsä, J., Method for the manufacture of olefins, *Patent WO 0 144 145*, Fortum Oil & Gas Oy, 21 June 2001.
- [67] Satta, A., Baklanov, M., Richard, O., Vantomme, A., Bender, H., Conard, T., Maex, K., Li, W. M., Elers, K. E. and Haukka, S., Enhancement of ALCVD (TM) TiN growth on Si–O–C and  $\alpha$ -SiC:H films by O<sub>2</sub>-based plasma treatments, *Microelectron. Eng.* **60** (2002) 59–69.
- [68] Drozd, V. E., Baraban, A. P. and Nikiforova, I. O., Electrical properties of Si–Al<sub>2</sub>O<sub>3</sub> structures grown by ML–ALE, *Appl. Surf. Sci.* **82/83** (1994) 583–586.
- [69] Ott, A. W., Klaus, J. W., Johnson, J. M. and George, S. M., Al<sub>2</sub>O<sub>3</sub> thin film growth on Si(100) using binary reaction sequence chemistry, *Thin Solid Films* **292** (1997) 135–144.
- [70] Van Der Voort, P. and Vansant, E. F., The creation of silicon nitride coatings by successive gas-phase reactions with trichlorosilane and ammonia. Chemical surface coating. A new route towards thin ceramic layers on silica, *Pol. J. Chem.* **70** (1996) 838–849.
- [71] Suntola, T. and Antson, J., Method for producing compound thin films, *Patent US 4 058 430*, 15 November 1977.
- [72] Suntola, T., Surface chemistry of materials deposition at atomic layer level, *Appl. Surf. Sci.* **100/101** (1996) 391–398.
- [73] Niinistö, L., Atomic layer epitaxy, *Curr. Opin. Solid State Mater. Sci.* **3** (1998) 147–152.
- [74] Kanervo, J. M. and Krause, A. O. I., Kinetic analysis of temperature-programmed reduction: behavior of a CrO<sub>x</sub>/Al<sub>2</sub>O<sub>3</sub> catalyst, *J. Phys. Chem. B* **105** (2001) 9778–9784.
- [75] Aarik, J., Aidla, A., Mändar, H. and Uustare, T., Atomic layer deposition of titanium dioxide from TiCl<sub>4</sub> and H<sub>2</sub>O: investigation of growth mechanism, *Appl. Surf. Sci.* **172** (2001) 148–158.

- [76] Putkonen, M., *Development of low-temperature deposition processes by atomic layer epitaxy for binary and ternary oxide thin films*, Doctoral thesis, Helsinki University of Technology, Espoo, 2002, 69 p.
- [77] Haukka, S. and Root, A., The reaction of hexamethyldisilazane and subsequent oxidation of trimethylsilyl groups on silica studied by solid-state NMR and FTIR, *J. Phys. Chem.* **98** (1994) 1695–1703.
- [78] Vansant, E. F., Van Der Voort, P. and Vrancken, K. C., *Characterization and chemical modification of the silica surface*, Vol. 93 of *Stud. Surf. Sci. Catal.*, Elsevier, Amsterdam 1995, 486 p.
- [79] Tsyganenko, A. A. and Mardilovich, P. P., Structure of alumina surfaces, *J. Chem. Soc., Faraday Trans.* **92** (1996) 4843–4852.
- [80] Kytökivi, A., Lakomaa, E.-L. and Root, A., Controlled formation of ZrO<sub>2</sub> in the reaction of ZrCl<sub>4</sub> vapor with porous silica and  $\gamma$ -alumina surface, *Langmuir* **12** (1996) 4395–4403.
- [81] Peglar, R. J., Hambleton, F. H. and Hockey, J. A., Surface structure and catalytic cracking properties of the SiO<sub>2</sub>/BCl<sub>3</sub>, SiO<sub>2</sub>/AlMe<sub>3</sub> and SiO<sub>2</sub>/AlCl<sub>3</sub> systems, *J. Catal.* **20** (1971) 309–320.
- [82] Bartram, M. E., Michalske, T. A. and Rogers, Jr., J. W., A reexamination of the chemisorption of trimethylaluminum on silica, *J. Phys. Chem.* **95** (1991) 4453–4463.
- [83] Lakomaa, E.-L., Root, A. and Suntola, T., Surface reactions in Al<sub>2</sub>O<sub>3</sub> growth from trimethylaluminium and water by atomic layer epitaxy, *Appl. Surf. Sci.* **107** (1996) 107–115.
- [84] Haukka, S., Lakomaa, E.-L. and Suntola, T., Chemisorption of chromium acetylacetonate on porous high surface area silica, *Appl. Surf. Sci.* **75** (1994) 220–227.
- [85] Hakuli, A. and Kytökivi, A., Binding of chromium acetylacetonate on a silica support, *Phys. Chem. Chem. Phys.* **1** (1999) 1607–1613.
- [86] Babich, I. V., Plyuto, Y. V., Van Der Voort, P. and Vansant, E. F., Thermal transformations of chromium acetylacetonate on silica surface, *J. Colloid Interface Sci.* **189** (1997) 144–150.

- [87] Lindblad, M. and Pakkanen, T. A., Surface model for ZnS thin-films—ZnS clusters and chemisorption of ZnCl<sub>2</sub> on ZnS surface, *J. Comput. Chem.* **9** (1988) 581–590.
- [88] Babich, I. V., Plyuto, Y. V., Van Der Voort, P. and Vansant, E. F., Gas-phase deposition and thermal transformations of Cr(acac)<sub>3</sub> on the surface of alumina supports, *J. Chem. Soc., Faraday Trans.* **93** (1997) 3191–3196.
- [89] Köhler, S., Reiche, M., Frobel, C. and Baerns, M., Preparation of catalysts by chemical vapor-phase deposition and decomposition on support materials in a fluidized-bed reactor, *Preparation of Catalysts VI. Proc. 6th Int. Symp. "Scientific Bases for the Preparation of Heterogeneous Catalysts," Louvain-la-Neuve, Belgium, September 1994*, Eds. G. Poncelet, J. Martens, B. Delmon, P. A. Jacobs and P. Grange, Vol. 91 of *Stud. Surf. Sci. Catal.*, Elsevier, Amsterdam 1995, pp. 1009–1016.
- [90] Haukka, S., Lakomaa, E.-L. and Root, A., An IR and NMR study of the chemisorption of TiCl<sub>4</sub> on silica, *J. Phys. Chem.* **97** (1993) 5085–5094.
- [91] Haukka, S., Lakomaa, E.-L., Jylhä, O., Vilhunen, J. and Hornytzkj, S., Dispersion and distribution of titanium species bound to silica from TiCl<sub>4</sub>, *Langmuir* **9** (1993) 3497–3506.
- [92] Haukka, S., *Characterization of surface species generated in atomic layer epitaxy on silica*, Doctoral thesis, University of Helsinki, 1993, 46 p.
- [93] Kytökivi, A., *Growth of ZrO<sub>2</sub> and CrO<sub>x</sub> on high surface area oxide supports by atomic layer epitaxy*, Doctoral thesis, Helsinki University of Technology, Espoo, 1997, 55 p.
- [94] Jussila, M., *The binding of yttrium and other rare earth β-diketonate complexes on silica and their application to thin film growth*, M.Sc. thesis, Helsinki University of Technology, Espoo, 1998, 101 p. In Finnish.
- [95] Uusitalo, A. M., Pakkanen, T. T., Kröger-Laukkanen, M., Niinistö, L., Hakala, K., Paavola, S. and Löfgren, B., Heterogenization of racemic ethylenebis(1-indenyl)zirconium dichloride on trimethylaluminum vapor modified silica surface, *J. Mol. Catal., A* **160** (2000) 343–356.
- [96] Likhbolov, V. A. and Moroz, B. L., Hydroformylation, In *Handbook of Heterogeneous Catalysis*, Eds. G. Ertl, H. Knözinger and J. Weitkamp, Vol. 5, VCH, Weinheim 1997, pp. 2231–2244.

- [97] Chuang, S. S. C. and Pien, S.-I., Infrared spectroscopic studies of ethylene hydroformylation on Rh/SiO<sub>2</sub>—an investigation of the relationships between homogeneous and heterogeneous hydroformylation, *J. Mol. Catal.* **55** (1989) 12–22.
- [98] Chuang, S. S. C. and Pien, S.-I., Role of silver promoter in carbon-monoxide hydrogenation and ethylene hydroformylation over Rh/SiO<sub>2</sub> catalysts, *J. Catal.* **138** (1992) 536–546.
- [99] Takahashi, N., Takeyama, T., Yanagibashi, T. and Takada, Y., Comparison of pentan-3-one formation with propionaldehyde formation during ethylene hydroformylation over Rh active-carbon catalyst, *J. Catal.* **136** (1992) 531–538.
- [100] Andersson, C., Nikitidis, A., Hjortkjær, J. and Heinrich, B., Continuous liquid-phase hydroformylation of 1-hexene with a poly-trim bound rhodium phosphine complex, *Appl. Catal., A* **96** (1993) 345–354.
- [101] Sachtler, W. M. H. and Ichikawa, M., Catalytic site requirements for elementary steps in syngas conversion to oxygenates over promoted rhodium, *J. Phys. Chem.* **90** (1986) 4752–4758.
- [102] Huang, L., Xu, Y. D., Guo, W. G., Liu, A. M., Li, D. M. and Guo, X. X., Study on catalysis by carbonyl cluster-derived SiO<sub>2</sub>-supported rhodium for ethylene hydroformylation, *Catal. Lett.* **32** (1995) 61–81.
- [103] Buonomo, F., Sanfilippo, D. and Trifiró, F., Dehydrogenation of alkanes, In *Handbook of Heterogeneous Catalysis*, Eds. G. Ertl, H. Knözinger and J. Weitkamp, Vol. 5, VCH, Weinheim 1997, pp. 2140–2151.
- [104] Weyten, H., Keizer, K., Kinoo, A., Luyten, J. and Leysen, R., Dehydrogenation of propane using a packed-bed catalytic membrane reactor, *AIChE J.* **43** (1997) 1819–1827.
- [105] Gryaznov, V. M., Ermilova, M. M. and Orekhova, N. V., Membrane-catalyst systems for selectivity improvement in dehydrogenation and hydrogenation reactions, *Catal. Today* **67** (2001) 185–188.
- [106] Weckhuysen, B. M. and Schoonheydt, R. A., Alkane dehydrogenation over supported chromium oxide catalysts, *Catal. Today* **51** (1999) 223–232.
- [107] De Rossi, S., Ferraris, G., Fremiotti, S., Garrone, E., Ghiotti, G., Campa, M. C. and Indovina, V., Propane dehydrogenation on chromia silica and chromia alumina catalysts, *J. Catal.* **148** (1994) 36–46.

- [108] Burwell, Jr., R. L., Littlewood, A. B., Cardew, M., Pass, G. and Stoddart, T. H., Reactions between hydrocarbons and deuterium on chromium oxide gel. I. General, *J. Am. Chem. Soc.* **82** (1960) 6272–6280.
- [109] Zwahlen, A. G. and Agnew, J. B., Isobutane dehydrogenation kinetics determination in a modified Berty gradientless reactor, *Ind. Eng. Chem. Res.* **31** (1992) 2088–2093.
- [110] Airaksinen, S. M. K., Harlin, M. E. and Krause, A. O. I., Kinetic modeling of dehydrogenation of isobutane on chromia–alumina catalyst, *Ind. Eng. Chem. Res.* in press.
- [111] Hakuli, A., Kytökivi, A., Krause, A. O. I. and Suntola, T., Initial activity of reduced chromia/alumina catalyst in *n*-butane dehydrogenation monitored by on-line FT–IR gas analysis, *J. Catal.* **161** (1996) 393–400.
- [112] Grzybowska, B., Słoczyński, J., Grabowski, R., Wcicło, K., Kozłowska, A., Stoch, J. and Zieliński, J., Chromium oxide/alumina catalysts in oxidative dehydrogenation of isobutane, *J. Catal.* **178** (1998) 687–700.
- [113] Cavani, F., Koutyrev, M., Trifirò, F., Bartolini, A., Ghisletti, D., Iezzi, R., Santucci, A. and Piero, G. D., Chemical and physical characterization of alumina-supported chromia-based catalysts and their activity in dehydrogenation of isobutane, *J. Catal.* **158** (1996) 236–250.
- [114] De Rossi, S., Pia Casaletto, M., Ferraris, G., Cimino, A. and Minelli, G., Chromia/zirconia catalysts with Cr content exceeding the monolayer. A comparison with chromia/alumina and chromia/silica for isobutane dehydrogenation, *Appl. Catal., A* **167** (1998) 257–270.
- [115] Lugo, H. J. and Lunsford, J. H., The dehydrogenation of ethane over chromium catalysts, *J. Catal.* **91** (1985) 155–166.
- [116] Hakuli, A., *Preparation and characterization of supported CrO<sub>x</sub> catalysts for butane dehydrogenation*, Doctoral thesis, Helsinki University of Technology, Espoo, 1999, 48 p.
- [117] Brückner, A., Simultaneous combination of in situ-EPR/UV–VIS/on line GC: a novel setup for investigating transition metal oxide catalysts under working conditions, *Chem. Commun.* (2001) 2122–2123.

- [118] Puurunen, R. L., Beheydt, B. G. and Weckhuysen, B. M., Monitoring chromia/alumina catalysts in situ during propane dehydrogenation by optical fiber UV-visible diffuse reflectance spectroscopy, *J. Catal.* **204** (2001) 253–257.
- [119] Puurunen, R. L. and Weckhuysen, B. M., Spectroscopic study on the irreversible deactivation of chromia/alumina dehydrogenation catalysts, *J. Catal.* **210** (2002) 418–430.
- [120] Kanervo, J. M. and Krause, A. O. I., Characterisation of supported chromium oxide catalysts by kinetic analysis of H<sub>2</sub>-TPR data, *J. Catal.* **207** (2002) 57–65.
- [121] Brückner, A., Radnik, J., Hoang, D.-L. and Lieske, H., In situ investigation of active sites in zirconia-supported chromium oxide catalysts during the aromatization of *n*-octane, *Catal. Lett.* **60** (1999) 183–189.
- [122] Yates, D. J. C., Dembinski, G. W., Kroll, W. R. and Elliott, J. J., Infrared studies of the reactions between silica and trimethylaluminum, *J. Phys. Chem.* **73** (1969) 911–921.
- [123] Murray, J., Sharp, M. J. and Hockey, J. A., The polymerization of propylene by the SiO<sub>2</sub>/TiCl<sub>4</sub>/AlMe<sub>3</sub> system, *J. Catal.* **18** (1970) 52–56.
- [124] Peglar, R. J., Murray, J., Hambleton, F. H., Sharp, M. J., Parker, A. J. and Hockey, J. A., Chemical production and trapping of methyl radicals at silica surfaces, *J. Chem. Soc. A* (1970) 2170–2172.
- [125] Kunawicz (née Murray), J., Jones, P. and Hockey, J. A., Reactions of silica surfaces with hydrogen sequestering agents, *Trans. Faraday Soc.* **67** (1971) 848–853.
- [126] Morrow, B. A. and Hardin, A. H., Raman spectra of some hydrogen sequestering agents chemisorbed on silica, *J. Phys. Chem.* **83** (1979) 3135–3141.
- [127] Low, M. J. D., Severdia, A. G. and Chan, J., Reactive silica. XV. Some properties of solids prepared by the reaction of trimethylaluminum with silica, *J. Catal.* **69** (1981) 384–391.
- [128] Kinney, J. B. and Staley, R. H., Reactions of titanium tetrachloride and trimethylaluminum at silica surfaces studied by using infrared photoacoustic spectroscopy, *J. Phys. Chem.* **87** (1983) 3735–3740.
- [129] Engelsberg, A. C., Chera, J. J. and Korenowski, G. M., Adsorbed TMA on dielectric oxide surfaces, *Mater. Res. Soc. Symp. Proc.* **101** (1988) 159–164.

- [130] Engelsberg, A. C., *Spectroscopic studies of trimethyl aluminum on silicon dioxide and aluminum oxide surfaces*, Doctoral thesis, Rensselaer Polytechnic Institute, Troy, NY, 1987, 163 p.
- [131] Morrow, B. A. and McFarlan, A. J., Chemical reactions at silica surfaces, *J. Non-Cryst. Solids* **120** (1990) 61–71.
- [132] Soto, C. and Tysoe, W. T., The reaction pathway for the growth of alumina on high surface area alumina and in ultrahigh vacuum by a reaction between trimethyl aluminum and water, *J. Vac. Sci. Technol., A* **9** (1991) 2686–2695.
- [133] Kratochvíla, J., Kadlc, Z., Kazda, A. and Salajka, Z., Reaction of silica gel with alkylaluminium compounds and with titanium tetrachloride, *J. Non-Cryst. Solids* **143** (1992) 14–20.
- [134] Soto, C., Wu, R., Bennett, D. W. and Tysoe, W. T., Infrared spectroscopy of trimethylaluminum and dimethylaluminum chloride adsorbed on alumina, *Chem. Mater.* **6** (1994) 1705–1711.
- [135] Morrow, B. A. and McFarlan, A. J., Infrared study of chemical and H–D exchange probes for silica surfaces, In *Colloid Chemistry of Silica*, Vol. 234 of *Adv. Chem. Ser.*, American Chemical Society, Washington 1994, pp. 183–198.
- [136] Dillon, A. C., Ott, A. W., Way, J. D. and George, S. M., Surface chemistry of Al<sub>2</sub>O<sub>3</sub> deposition using Al(CH<sub>3</sub>)<sub>3</sub> and H<sub>2</sub>O in a binary reaction sequence, *Surf. Sci.* **322** (1995) 230–242.
- [137] Anwander, R., Palm, C., Groeger, O. and Engelhardt, G., Formation of Lewis acidic support materials via chemisorption of trimethylaluminum on mesoporous silicate MCM-41, *Organometallics* **17** (1998) 2027–2036.
- [138] Juppo, M., Rahtu, A., Ritala, M. and Leskelä, M., In situ mass spectrometry study on surface reactions in atomic layer deposition of Al<sub>2</sub>O<sub>3</sub> thin films from trimethylaluminum and water, *Langmuir* **16** (2000) 4034–4039.
- [139] Juppo, M., *Atomic layer deposition of metal and transition metal nitride thin films and in situ mass spectrometry studies*, Doctoral thesis, University of Helsinki, 2001, 65 p.
- [140] Rahtu, A., Alaranta, T. and Ritala, M., In situ quartz crystal microbalance and quadrupole mass spectrometry studies of atomic layer deposition of aluminum oxide from trimethylaluminum and water, *Langmuir* **17** (2001) 6506–6509.

- [141] Rahtu, A., *Atomic layer deposition of high permittivity oxides: film growth and in situ studies*, Doctoral thesis, University of Helsinki, 2002, 69 p.
- [142] Apblett, A. W. and Barron, A. R., Cleavage of poly(diorganosiloxanes) by trimethylaluminum, *Organometallics* **9** (1990) 2137–2141.
- [143] Cotton, F. A. and Wilkinson, G., *Basic Inorganic Chemistry*, John Wiley & Sons, New York 1976. p. 88.
- [144] Puurunen, R. L., Effect of the size and reactivity of the metal reactant ( $ML_n$ ) on ALD growth, *AVS Topical Conference on Atomic Layer Deposition "ALD 2002," Seoul, Korea, August 2002*, oral presentation, Book of Abstracts, p. 31.
- [145] Ylilammi, M., Monolayer thickness in atomic layer deposition, *Thin Solid Films* **279** (1996) 124–130.
- [146] Brongersma, H. H., Groenen, P. A. C. and Jacobs, J.-P., Application of low energy ion scattering to oxidic surfaces, In *Science of Ceramic Interfaces II*, Ed. J. Nowotny, Vol. 81 of *Mater. Sci. Monographs*, Elsevier, Amsterdam 1994, pp. 113–182.
- [147] Rodgers, G. E., *Introduction to coordination, solid state, and descriptive inorganic chemistry*, McGraw-Hill, Singapore 1994. p. 164.
- [148] Nieminen, M., *Deposition of binary and ternary oxide thin films of trivalent metals by atomic layer epitaxy*, Doctoral thesis, Helsinki University of Technology, Espoo, 2001, 57 p.
- [149] Utriainen, M., Kröger-Laukkanen, M. and Niinistö, L., Studies of NiO thin film formation by atomic layer epitaxy, *Mater. Sci. Eng., B* **54** (1998) 98–103.
- [150] Jacobs, J. P., Lindfors, L. P., Reintjes, J. G. H., Jylhä, O. and Brongersma, H. H., The growth-mechanism of nickel in the preparation of Ni/Al<sub>2</sub>O<sub>3</sub> catalysts studied by LEIS, XPS and catalytic activity, *Catal. Lett.* **25** (1994) 315–324.
- [151] Haukka, S., Lindblad, M. and Suntola, T., Growth mechanisms of mixed oxides on alumina, *Appl. Surf. Sci.* **112** (1997) 23–29.
- [152] Kenvin, J. C., White, M. G. and Mitchell, M. B., Preparation and characterization of supported mononuclear metal-complexes as model catalysts, *Langmuir* **7** (1991) 1198–1205.

- [153] Kytökivi, A., Rautiainen, A. and Root, A., Reaction of acetylacetone vapour with  $\gamma$ -alumina, *J. Chem. Soc., Faraday Trans.* **93** (1997) 4079–4084.
- [154] Babich, I. V., Plyuto, Y. V., Van Langeveld, A. D. and Moulijn, J. A., Role of the support nature in chemisorption of  $\text{Ni}(\text{acac})_2$  on the surface of silica and alumina, *Appl. Surf. Sci.* **115** (1997) 267–272.